Field and Laboratory Measurement of Radon Flux and Diffusion for Uranium Mill Tailings Cover Systems

By

Nick Stefani

A Thesis submitted in partial fulfillment of the requirements for the degree of

Master of Science

(Geological Engineering)

at the

UNIVERSITY OF WISCONSIN-MADISON

2016

MASTER OF SCIENCE

(Geological Engineering)

At the

UNIVERSITY OF WISCONSIN-MADISON

2016

Approved by:

William J. Likos, PhD

ABSTRACT

Disposal Facilities for uranium mill tailings have been constructed as required by the Uranium Mine Tailing Radiation Control Act (UMTRCA) of 1978. Nearly all of these facilities rely on a low-permeability, compacted clay surface cover to control the rate at which contaminants migrate in the gas and water phase from the tailings into the environment. The primary engineered component of the surface cover is typically referred to as the “low permeability Radon barrier, (or Rn Barrier). The Rn Barrier is designed to have low hydraulic conductivity and low gaseous diffusivity to effectivity control the emission of Radon and other contaminants into the environment.

Several of the UMTRCA sites are over 20 years of service life. It is well understood that near-surface clay covers can experience significant structure development (e.g., cracking) due to process related to environmental exposure, including seasonal wetting and drying and bio-intrusion from vegetation and animal activity. Over many seasons, there is the potential that the Rn Barrier system may not contain contaminants as well as when the barrier was initially constructed. Studies conducted on UMTRCA sites have indicated significant variability in Radon Flux (Rn Flux) emanating through the top of the Rn Barrier (e.g., from as little as 0.3 pCi/m^2-s to as much as 200 pCi/m^2-s) (CNWRA 2012). When UMTRCA was first passed, the intended service life of cover systems was 1,000 years and Rn Flux was stipulated to not exceed 20 pCi/m^2-s.

This study first seeks to develop and calibrate alternative measurement techniques for accurately and reliably measuring Rn Flux at UMTRCA field sites. The study is motivated partly to address limitations in current regulatory measurement techniques, where Radon surface flux is measured using Activated Carbon (AC) placed directly on the cover surface and Radon is measured by passive sorption. Advances in Radon measurement technologies have led to the development of continuous, electronic Radon monitors. These monitors are capable of measuring Radon concentration at user-specified intervals and thus can be used to measure the buildup of

Radon inside a closed sampling chamber placed on the cover system over time. Continuous data afforded by this approach provides significant advantages for measuring Rn flux over the historical AC measurement approach. The calibration effort of this study employed an electronic RAD7 Radon detection system (Durridge Company Inc.) to measure Rn flux emanating from two Radon sources in the laboratory (granite aggregate and a poured concrete slab). Results were used to develop an experimental protocol for field measurements and to identify and characterize variables that affect the measurements.

AC canisters were placed into chambers containing the Radon sources in tandem with the electronic radon monitors so that radon concentrations measured using the two approaches could be directly compared. The AC to RAD7 Rn Concentration ratio averaged 0.58 (+/- 0.07) for five tests under the same conditions. A second suite of experiments was conducted to examine the effects of process variables on the measurements, including relative humidity, chamber size, exposure duration, and Rn flux. Similar differences in the two techniques were observed. The lab analysis properly corrected varying levels of exposure to RH before Rn exposure to the same Rn concentration (198.5 +/- 23.8 Bq/m3), but that concentration consistently averaged 0.60 (+/- 0.07) in the AC to RAD7 Rn Concentration Ratio. Varying chamber size, Rn flux, and exposure time all failed to produce statistically significant trends with R^2 = 0.73, 0.42, and 0.28 respectively.

Field measurements were conducted at a uranium mill tailings disposal cell located in Falls City, Texas. Continuous (RAD7) and passive (AC canisters) Radon detectors were deployed at six test pits that were excavated to expose the Rn barrier at the site and to measure radon flux at locations representative of different site conditions. Test pit locations were selected to compare varying vegetation conditions, Rn barrier thicknesses, and underlying tailings activities. Rn flux measured at the top of the barrier within the six test pits ranged from 0.06 - 24.74 pCi/m^2-s. Radon flux measurements were also conducted directly on top of the tailings layer, which was exposed by excavating through the Rn Barrier. Radon flux from the tailings layer was measured as high

as 1148.07 pCi/m^2-s. Results from this suite of measurements were used to assess performance of the alternative Radon measurement approaches in a typical field application. The AC to RAD7 Rn concentration ratio was consistent with the laboratory measurements, averaging 0.59 with a variance of 0.07. Corresponding ratio of Rn flux between the two devices was 0.60-0.93 depending on the size of the chamber and length of the test.

Finally, a laboratory procedure was developed to simulate desiccation and structure development inside compacted clay samples and the associated effects on gaseous Radon diffusion coefficient. Experiments were conducted in a modified flexible wall permeameters to measure Radon diffusion coefficients through several wetting and drying cycles. Results were used to understand how structure develops in different types of clays that may be considered representative of compacted cover materials and to quantify the associated effects on Radon diffusivity. Measured Rn diffusion coefficients across all clays ranged from a maximum of 3.98e-7 m^2/s to a minimum of 1.24e-09 m^2/s. These values fall within the expected diffusion coefficients boundaries of air (1e-5 m^2/s) and water (1e-9 m^2/s).

ACKNOWLEDGEMENTS

The UW-Madison Geological Engineering Department has been a fantastic home for the past two years of my Master's Degree work. The professors, staff, and other graduate students have been incredibly helpful in guiding my personal growth and professional development. Together, they have taught me engineering fundamentals, critical thinking skills, writing proficiency, and presentation skills.

First, I must thank my advisor, Professor Bill Likos. He provided me with my first taste of academic research when I was still and undergraduate and to offer an opportunity to pursue a Master's Degree in Geological Engineering. Professor Likos has been extremely helpful in pushing my critical thinking, creative thinking and engineering skills on a day to day basis. In addition he has fermented a wonderful environment for me to explore my personal and engineering interests. Thanks must also be extended to Professor Benson, who has continually pushed me to be a better engineer, presenter, and writer. I would also like to thank Professor Edil for following this research progress, providing his input and serving on my committee.

Supplementary help and appreciation must also be extended to other groups that made this research possible; Professor Phil Brown of the UW Geoscience and Tom Elias of Johnson and Johnson Mining Company for willingness to help acquire a Radon source, Victor Gortesky and Yulia Henes for helping identify potential safety issues, loaning a RAD7 unit, and providing helpful advice in the early stages of the project, Dr. Danta Galan of RTCA for sharing data and laboratory procedures to better understand the underlying phenomena at work, which proved to be more than critical, Professor Robert McTaggert of South Dakota State University for loaning and additional RAD7 unit and unmeasurable advice, guidance, and patience must be extended to Xiadong "Buff" Wang, head of the GLE Soils Lab, for assistance in laboratory work and field measurements related to the project.

Finally, friends and family in and out of the GLE department must be thanked for helping progress this project and aiding my Master's Degree work, and providing the support I needed to successfully conclude my work.

Financial support for this study is from the University of Wisconsin – Madison, The Legacy Management of the Department of Energy and The Nuclear Regulatory Commission. This support is gratefully acknowledged. The findings and recommendations that have been presented are solely those of the author, and do not necessarily represent the policies or opinions of the sponsors.

TABLE OF CONTENTS

LIST OF TABLES

LIST OF FIGURES

CHAPTER 1

LABORATORY CALIBRATION OF ELECTRONIC AND ACTIVATED CARBON METHODS TO MEASURE RADON FLUX IN SURFACE COVER APPLICATIONS

1.1. INTRODUCTION

Continuous electronic Radon monitors are a relatively new development in the radon measurement field (Ferry et al. 2002; ORAU 2014). By employing a solid state alpha detector, they can measure the concentration of radon inside a closed chamber at discrete intervals over long periods of time. Through this method, the buildup in the concentration of radon (buildup curve) can be recorded and used to calculate an initial flux of radon emanating from the source. Such monitors have also been widely used in academic lab work. One common application is measuring emanation rates of common building and architectural materials, like concrete and granite, to predict the indoor concentration of radon in residential or commercial environments (e.g., basements). These monitors have proven to be reliable and useful for calculating radon fluxes.

This study aims to adapt a continuous radon monitoring method for field measurements of Radon flux (Rn flux) through clay covers on UMTRCA sites. The calibration and calculation process is described for conducting Rn flux measurements on a surface emanating radon. Current UMTRCA measurement techniques (activated carbon canisters) are directly compared to results obtained using the RAD7 approach to assess differences, advantages, and potential issues between the two processes.

1.2. BACKGROUND

Rn barriers at UMTRCA facilities are evaluated immediately after construction to determine if they meet the Rn flux requirement. Current practice involves deployment of an activated carbon (AC)

canister placed directly on top of the Rn barrier for about 24 h in a flux accumulator with an area equal to 0.071 m^2 (Figure 1.1). Sorption of Radon on the carbon surface occurs in the gas phase. After some time, the carbon inside the chamber is analyzed for counts of radon, which may be calculated into an Rn flux. Rn flux is stipulated by UMTRCA to be less than 2664 Bq/m^2-h (20 pCi/m^2-s) (UMTRCA 2013). The AC procedure is simple, low-cost and can be repeated numerously over a large (several acre) UMTRCA disposal cell.

The Center for Nuclear Waste Regulatory Analyses (2012) conducted Rn flux measurements on Rn barriers using passive AC samplers over several years in an attempt to understand how Rn flux changes temporally, seasonally, annually, and over the life of UMTRCA clay covers. Significant variations in measured Rn flux were observed for measurements conducted over a six year period. Over just one year, Rn flux measured using the AC canister approach was as high as 26,640 Bq/m^2-h (200 pCi/m^2-s) and as low as 39.9 Bq/m^2-h (0.3 pCi/m^2-s). While, some variation may be attributable to variation in environmental factors that limit or enhance Rn flux (e.g., water saturation of the Rn barrier and ambient air pressure), significant scatter in the results motivates effort to understand sources of uncertainty in the measurement approach and to explore alternative measurement approaches for application at UMTRCA sites.

Uncertainty in the AC measurement approach arises from several potential sources. The activated carbon measurement approach is a sorption based, passive measurement technique. Accuracy of the accumulated radon count is affected by the presence of water vapor in the sensing chamber, which can reduce sorption sites available on the AC that are otherwise available for radon (Vargas and Ortega 2007). Correction factors designed for lab analysis may be improperly calculated for flux chambers that buildup radon. Additionally, final covers for UMTRCA facilities are designed to have an indefinite service life. Degradation of the Rn barrier can occur over long periods of time (Suter 1993; Benson et. al. 2007, 2011; Waugh et. al. 2015). Freeze-thaw and wet-dry cycling of compacted clay barriers are known to cause increases in

saturated hydraulic conductivity of several orders of magnitude (Benson and Othman 1993; Othman et. al. 1994, Benson et. al. 1995; Albrecht and Benson 2001; Albright el al. 2006 a, b). Rn fluxes are likely affected similarly, changing the amount of radon diffusing from the tailings into the environment.

1.3. MATERIALS

1.3.1. Radon Sources

Radon sources were obtained to provide consistent and measurable Rn flux for sensor calibration. Materials with low levels of Radon emanation were required to simulate typical Radon Fluxes consistent with UMTRCA site conditions. Radon Fluxes as low as 39.9 Bq/m^2-h (0.3 pCi/m^2-s), for example, have been measured with Activated Carbon on UMTRCA cells.

The first source used in this study was Wisconsin Red Granite. Wisconsin Red Granite is found in North Central Wisconsin and used in monument stone, landscape, and other applications. When mined, the crushed granite is sieved and separated into different grain sizes. For this study, Red Granite was selected from a span of grain sizes from 40 mm to 4.75 mm. Radon emanation of a granitic material is highly variable because the content of the father decay progeny (Uranium) can be highly variable from location to location within the rock formation (Chao et al. 1997).

It has also been observed that concrete can emanate low levels of Radon (Daoud and Renken 1999). If the natural material used to make up the concrete aggregate contains high enough levels of Uranium, concrete slabs will produce Radon flux at levels similar to levels expected at UMTRCA cells. Likewise, if the concrete contains a significant degree of cracking, radon may diffuse from the underlying surface through a concrete floor slab. The Computer Aided Engineering Building basement at the University of Wisconsin-Madison campus was the

laboratory for Rn flux measurements and also has a poured concrete slab as its floor. It was also used as a source material for laboratory measurements.

1.3.2. Activated Carbon (AC) Canisters

AC canisters are based on passive sorption of gaseous radon onto granular activated carbon (Gervino et al. 2004). After a period of exposure (e.g., placement of the canister in a closed environment), the canister is sealed and shipped to a laboratory for analysis. AC canisters can be deployed for less than a day to a week for short term tests, or for long term tests that could last 90 days to a year. The amount of adsorbed Rn is measured (e.g., by counting with a sodium iodide detector) and corresponding Rn concentration is calculated according to

$$RnC = \frac{(CR-BR)}{(E*C*t*\lambda)} \quad (1)$$

where *CR* is the counting rate (counts/min). *BR* is the background rate (counts/min). *E* is the efficiency (unit less) of the machine used and is calibrated each day by the lab. *C* is the calibration factor (counts/pCi-min/L). This value is derived from numerous tests calibrating the AC canister to a known Rn concentration and measured moisture gained. The time of exposure (min) is *t*. Finally, λ is the decay factor (1/min) that accounts for the amount of time from the end of exposure to the time of measurement in the laboratory. Equation (1) used in this study comes from the Radon Testing Corporation of America (Elmsford, NY) but the method to convert counts of Radon into a concentration or flux is similar to that used in other studies (Hartley and Freeman 1985).

The AC canisters used in this study were 100 mm diameter open-faced charcoal canisters (Figure 1.1) obtained from the Radon Testing Corporation of America (RTCA). They contained 90 g of AC. The National Radon Safety Board device code is 10331. Laboratory analysis was conducted and reported back by RTCA.

1.3.3. Electronic Radon Monitor

Continuous Electronic Radon monitors contain a solid state alpha defector to measure disintegrations of alpha progenies of Radon over a designated time period. The detector used in this study was the RAD7 (Durridge Company, Inc. Billerica, MA) (Figure 1.2), which has been used extensively in other studies of Rn exhalation (flux) rates from building materials such as granite and concrete (Chao et al. 1997: Tuccimei et al. 2006: Ujic et al. 2008). A pump in the RAD7 continually cycles air from the sampling environment (e.g., closed chamber) through the detector to distinguish between different energy levels so that only Radon is measured. A pump flow rate of 800 mL/min and a sampling frequency (cycle time) of one hour were used for all tests reported in this study. Measured counts of Radon during buildup in the sampling chamber are then calculated into a corresponding concentration. Monotonic increase in Rn concentration can be used to quantify an initial Radon flux from the source into the chamber.

1.3.4. Flux Chambers

Different sized sampling chambers were used to assess any effects that scale may have on Radon flux measurements using the AC and RAD7 measurement approaches. Four sizes were selected with different flux areas (A). These are designated herein as large, medium, small, and extra small. Flux area is defined as the projected cross-sectional area of the Rn source material exposed to the flux chamber, and is equal to the cross-sectional area of the chamber. The large chamber (1.5 m x 1.5 m square cross section, A = 2.32 m^2, V = 0.352 m^3) was adapted from the sealed double ring infiltrometer (SDRI) measurement technique to measure large scale field hydraulic conductivities (ASTM D5093 - 15). The medium chamber was a rectangular HDPE container (A = 0.590 m^2, V = 0.204 m^3). The small chamber was a 0.3 m diameter circular polyvinyl chloride (PVC) end cap (A = 0.071 m^2, V = 0.011 m^3) and resembles the same dimensions and design of the flux chamber used in the CNWRA report in 2012 that measured Rn flux with AC over a six-year period. This construction is also most commonly used in UMTRCA guidelines for

the post construction Rn flux measurements for compliance once the Rn barrier is completed. Lastly, the extra small chamber was a 0.15 m diameter circular polyvinyl chloride (PVC) end cap (A = 0.017 m^2, V = 0.002 m^3). A scaled image containing the dimensions in plan view and in cross section can be found in Figure 1.3.

Two holes were drilled in the top surface of the flux chambers and fitted with air tight ports used to attach tubing that would connect the RAD7 to the flux chamber. When the granite aggregate was used as an Rn source, a polyethylene sheet (25 µm thick) was placed between the granite and the concrete floor slab to minimize back diffusion of Rn into the concrete, as well as transmission of Rn from the concrete. When the concrete slab was used as the Rn source, the chamber was placed directly on top of the slab with no polyethylene sheet. For laboratory tests, the chamber (interface between the chamber edge and floor surface) was sealed with duct tape to prevent Rn leakage from the chamber. Figure 1.4 contains a schematic of the experimental set up.

1.4. METHODS

1.4.1. Theory for Calculating Rn Flux

1.4.1.1. Theory for Continuous Rn Monitor Data (RAD7)

Transient Rn concentration in a closed flux chamber containing a constant Rn source can be modeled by considering mass balance of the system (Chao et al. 1997; Tuccimei et al. 2006; Ujic et al. 2008):

$$\frac{dC}{dt} = -\lambda C - DC + \frac{J_o A}{V} + \frac{q(Co-C)}{V} \quad (2)$$

where C (Bq/m^3) is Rn concentration, t (h) is time, λ (1/h) is a decay coefficient, D (1/h) is the back diffusion coefficient, J_0 (Bq/m^2-h) is initial Rn flux into the flux chamber, A (m^2) is the flux area of the chamber, V (m^3) is the volume of the chamber, q (1/h) is a leakage coefficient, and C_0 is the

background (e.g., ambient) Rn concentration. The decay term is necessary because of the short half-life of Rn (3.8 d). For an unvented chamber, the back-diffusion term accounts for diffusion of Rn back into the source material as the concentration builds up inside the chamber. *Jo* is the radon emanating from the source into the chamber at time zero (before any back diffusion). The right-most term in Eq. 2 is used to quantify leakage of Rn from the chamber.

Eq. 2 is solved with the initial conditions $t = 0$ and $C = C_i$, to yield

$$C = \left(C_i - \frac{J_o A + qC_o}{V(\lambda_{eff})}\right)\left(1 - e^{-(\lambda_{eff} * t)}\right) + \frac{J_o A + qC_o}{V(\lambda_{eff})} \quad (3)$$

where

$$\lambda_{eff} = \lambda + D + \frac{q}{V} \quad (4)$$

Eq. 3 is fit to the Rn build up curve using least-squares analysis by adjusting J_o, and λ_{eff}.

If back diffusion is not significant (e.g., early in the measurement period), the initial slope (M_e) of the curve relating Rn concentration inside the chamber and time can be used to estimate the initial flux (J_o) from Eqs. 5 and 6.

$$\frac{dC}{dt}_{t \to 0} = M_e = \frac{J_o A + qC_o}{V} \quad (5)$$

$$J_o = \left(M_e - \frac{q}{V} C_o\right)\left(\frac{V}{A}\right) \quad (6)$$

For each Rn buildup curve, the optimization method and M_e method were averaged, producing the flux reported for each test.

1.4.1.2. Determining M_e

M_e was calculated by averaging three different methods. First, linear regression was conducted for each data point. Meaning for t = 5 h, linear regression was conducted from t = 1 h to t = 5 h.

This was continued for the entire buildup curve. Plotting the slope values from regression, an initial slope can be estimated. With measured data, there are typically three different zones of slope values (Figure 1.5). One where the noise between the first few data points produces erroneous slopes (1.5.a), one where the slopes values are flat and somewhat constant (no back diffusion effects, (1.5.b)), and one where the slope slowly decreases, trending to zero if given enough time (approaching equilibrium (1.5.c)). In the current study, the values in the second zone were averaged to calculate a representative M_e.

Additionally, each x-y pair of data in the buildup curve can be manipulated to estimate M_e. Each pair can be plotted y/x or x/y over time for the length of the buildup. Linear regression over the ending portions of the curves can be extrapolated back to the y-axis to approximate M_e, two different ways. These two approaches can be extremely difficult to interpret with fewer data points (<10), particularly noisy data, or data that do not capture enough of the curved induced by back diffusion. Caution and care must be exercised in interpreting the y/x and x/y curves, but it does provide a systematic procedure to estimate M_e.

Generally, the three approaches agreed well with each other and rarely varied enough to have a significant impact on the final calculated flux. Typically, the three never varied more than 15 Bq/m3-h from each other, a nearly insignificant difference after Rn flux is calculated. The M_e used to calculate J_o in Equation 2 and 6 was the average of the three different methods.

1.4.1.3. Theory for Passive Measurement Data (AC)

AC flux measurements are calculated by assuming the buildup of Rn in the chamber is constant and that all Rn is passively collected into the granular carbon. Using this assumption, the concentration of the AC canister can be converted to a flux with Eq. 7 below. This approach is identical to the M_e approach to calculate J_o for RAD7 data.

$$J = (\frac{C}{t})(\frac{V}{A}) \quad (7)$$

J is equal to Rn Flux (Bq/m^2-h), *C* is the Rn concentration (Bq/m^3), *t* is time (h), *V* is the volume of the flux chamber (m^3) and *A* is the flux chamber area (m^2). Not all cases are appropriate to use this approach. Eq. 7 can only be used as long as the Rn flux into the chamber is constant over the time of the measurement. Current UMTRCA guidelines stipulate that measurements should be conducted for 24 h, to avoid this complication. The magnitude of the flux and the chamber dimensions dictate when the Rn flux has ceased being constant and will be discussed further.

1.4.2. Source Radon Flux

Each of the four sized chambers was tested several times over a several month period. After each test, a flux was calculated. Both the parameter fitting and initial slope method were used to calculate Rn Flux. The average of the two was reported as Rn flux for each test. Test durations ranged from 18 to 96 h. A cycle time of 1 h was selected. Based on other studies, 1 h cycling was determined to maximize the amount of data while limiting uncertainty in the Rn concentration calculation. After each test, the chamber was purged or vented and resealed so that the next test would have a starting Rn concentration as close to zero as possible. When granite was tested, a constant ratio of granite mass to flux area (22.6 kg/m2) was maintained to maintain as consistent flux as possible throughout testing for each chamber. This ratio created a layer about 30 mm thick on top of the plastic sheeting on top of the ground surface, the concrete slab. Chambers were simply placed on top of the slab when concrete was tested.

1.4.3. Direct Comparison between AC and RAD7 Techniques in the Same Chamber

AC canisters were placed directly on top of the source surface (concrete slab or granite aggregate) and exposed during the same time the RAD7 sampled Rn in the chamber. Initially, five tests were run under identical conditions to establish a baseline. Tests were conducted with

the large (A = 2.32 m^2) chamber, a layer of granite and no plastic sheeting, which produced a consistent flux of 6.0 Bq/m^2-h, and 48 h exposure time. Next, several variables were altered to observe any differences in measured Radon between the two techniques. The flux area, magnitude of flux, and time of exposure were all varied to observe any differences in measured Rn between AC and RAD7 methods.

1.4.4. Effects of water vapor exposure on AC measurements

AC canisters were pre exposed to varying relative humidity (RH) conditions to determine the effects of water vapor exposure on Radon measurements using AC measurement approach. Two canisters were placed in sealed containers (0.004 m^3) with different super saturated salt solutions to produce RH ranging from 10 to 90% RH at 10% intervals (Figure 1.6). The AC canisters were allowed to equilibrate for 2 d in the controlled vapor pressure environments and were then all placed simultaneously inside the large chamber with a layer of granite and no plastic sheeting (Figure 1.7). The canisters were then sent to RTCA to be analyzed for the amount of moisture gained and Rn concentration to be compared directly to the buildup measured by the RAD7.

1.5. RESULTS

1.5.1. Concentration Buildup Curves

A total of 32 tests to measure Radon concentration buildup curves were run using the granite source and 28 tests were run using the concrete source. Examples of concentration build up curves from each chamber size with the granite aggregate as the Rn source are shown in Figure 1.4. The dashed tangent lines estimate the initial slope (M_e) using a manual curve fitting approach. Solid lines are best fit curves obtained by least-squared regression by optimizing J_o and λ_{eff}. Results from the entire suite of tests are summarized in Table 1.1 for the concrete and in Table 1.2. for the granite.

Tests using all four chamber sizes yielded an average Rn Flux of 3.23 Bq/m^2-h for Wisconsin Red Granite and 4.89 Bq/m^2-h for the concrete slab. These values are in good agreement with other data sets for other types of rock (Chao et al. 1997; Chao and Tung 1999; Tuccimei et al. 2006), as summarized in Table 1.3.

Results show that the dimensions of the chamber have an effect on the shape and timing of the buildup curve. As illustrated in Figure 1.8, the equilibrium concentration and the time to approach that equilibrium systematically increases as the chamber size increases. The large, small, and extra small chambers all have similar volume to area ratios (0.15, 0.15, and 0.11 respectively), so they can be compared directly (Figure 1.9). The medium chamber has a smaller volume to area ratio (0.35), and has a differently shaped buildup (Figure 1.10). In general, it takes longer to reach equilibrium and has a lower initial slope to the other chamber sizes (Figure 1.6). This difference is inconsequential for calculating initial Rn fluxes from the RAD7 data using either the manual slope fitting method or least squares regression. As discussed later, however, this effect can be problematic for AC canister measurements where the buildup of Radon is assumed to be linear with time during the duration of exposure.

Back diffusion coefficients (D) calculated from regression of for each test are also presented in Table 1.1. and 1.2. for concrete and granite respectively. *D* cannot be averaged over each test because not all tests were run to the point where back diffusion took place. Tests that were run for less than 24 h in the large chamber, for example, do not show evidence of back diffusion in the buildup curves and the corresponding buildup curve is linear. When J_o and C_{equ} are optimized, *D* is effectively zero. One test for each the granite and concrete that did run for a sufficient time to calculate *D* is presented in Table 1.3. Results for other measured values from similar materials from other studies are in good agreement.

1.5.2. Effect of Scale (Chamber Size)

Scaling effects were observed in comparisons of results for tests conducted using different chamber sizes. Rn fluxes are plotted as a function of flux area in Figure 1.7. for granite and concrete. Average Rn fluxes for each chamber (open squares) are similar for the large, medium, small, and extra small chambers. There is a general trend indicating that larger chamber sizes result in less variation from the average (dashed lines on Fig. 1.11). The population standard deviation for tests conducted using concrete is 1.13, 1.52, 0.66, and 0.64 for the extra small, small, medium and large chamber sizes, respectively. For granite, these values are 1.88, 1.11, 0.32, and 1.01. The medium chamber population standard deviation of 0.32 is much lower and not as representative of the overall trend because there was only three tests. The reduction in variability with increasing chamber size is interpreted to reflect increasing spatial averaging of small scale variations in flux (Vanmarcke 1983, Benson 1991).

Variations in measured Rn flux values over time are affected by temperature, air pressure, and heterogeneity in the source material (Countess 1976). It is expected that at the low levels of radioactivity considered here, those factors play a significant part in the differences observed in measured Rn flux. Likewise, variability in calculated Rn concentrations from the RAD7 would lead to slight variations in calculated Rn flux over many tests. For field measurements on compacted clay covers, the scaling effect may be more pronounced due to the presence of soil structure.

1.5.3. Direct Comparison of RAD7 and AC Results

A set of five control tests was first conducted over similar testing conditions to measure the variance in AC canister measurements. *Jo*, *A*, and time of exposure (*T*) were 6.0 Bq/m^2-h, 2.323 m^2, and 48 h. The AC canister value averaged 42.0% +/- 7.2% less than RAD7 measured values. Similarly, the RAD7 to AC Rn concentration ratio averaged 0.58. Figure 1.12 shows the RAD7 buildup curves with the single large point being the AC value.

Jo, *A*, and *T* was varied from 0.5 – 6.5 Bq/m^2-h, 0.018 – 2.323 m^2, and 12 – 96 h. The results of these tests are summarized in Table 1.4, which includes the AC to RAD7 Rn concentration. Only in tests were *A* and J_o was varied (Figure 1.13 and Figure 1.14) was there a noticeable trend. However, linear regression of the varied J_o data produced an $R^2 = 0.42$ and the standard deviation of five tests run under the same conditions was 0.044. Both indicate that increasing the flux is not statistically significant in altering the RAD7 to AC Rn concentration ratio. For the varied *A* data, regression produced a $R^2 = 0.73$, but there is not enough data to have confidence that a true trend exists. More testing is required. The data from varying *T* is pretend in Figure 1.15.

The difference between the two techniques appears to be systematic and independent of changes in *Jo*, *A*, and *T*. It is likely that there is a kinetic factor that must be corrected to better match the AC canister value to the value inside the flux chamber. A final test was conducted to maximize the exposure to Radon after the flux chamber was at a constant equilibrium. Four tests were run in the small flux chambers where the total time of exposure was be 4, 5, 6, and 7 d. 7 d was the maximum time of exposure recommended by RTCA to calculate Rn concentration.

The same variability in the average AC to RAD7 Rn concentration ratio for the 4, 5, 6, and 7 d tests was observed, 0.65. Figure 1.16 also shows that the 5 and 6 d tests show an increase in Rn concentration near the end of the test. This increase in Radon may be attributed to changes in air pressure or temperature. This compromises the underlying assumptions in this test's objective and limits its use in determining if at any point the two measurement techniques will have measured values will less than the spread of 0.48-0.83 RAD7 to AC Rn concentration ratio.

Despite this, it is much more likely that there is a systematic issue in directly comparing with AC canisters and RAD7 methods. The AC canisters are constructed and measured for residential use. The sampling environment (typically a basement) is assumed to be essentially

constant over the exposure time. The flux chambers used in this study have vastly different volumes and build up Rn concentration during exposure. It is expected that these factors create a systematic error in the correction factors used by RTCA.

1.5.4. Effects of Pre-exposure to Water Vapor

The AC canisters pre exposed to water vapor under controlled RH conditions displayed a clear trend of increasing moisture gained with increasing humidity (Figure 1.17). Water vapor competes with Radon to occupy sorption sites on the activated carbon (Vargas and Ortega 2007) and as expected in Figure 1.18, the net counts of measured radon for each canister decreases as RH was increased. RTCA's calibration factor is designed to correct for any moisture gained. All AC canisters were corrected to a narrow range of radon concentrations. The maximum value was 218.5 Bq/m^3, the minimum value was 174.4 Bq/m^3, and the average was 198.5 Bq/m^3. Based on other AC and RAD7 observations, this is a small band of difference.

While the corrections all lead to a consistent value, that value still did not measure the same level of radon built up inside the flux chamber. Figure 1.19 presents the RAD7 buildup curve for the flux chamber that all AC canisters were exposed to. The average AC canister value still had an AC to RAD7 Rn concentration ratio of 0.60, which is consistent with the previously discussed AC-RAD7 tandem tests. While RH does play a role in passive sorption, the corrections used in the lab analysis do account for it consistently, however they do not correct to the same RAD7 measured Rn concentration.

1.6. SUMMARY AND CONCLUSIONS

This laboratory and mass balance calculation approach has been properly adapted to measure Rn flux. Measured and calculated flux values of the two source materials yielded Rn fluxes of 3.32 and 4.89 Bq/m^2-h for Wisconsin Red granite and a common concrete slab. These values are in good agreement with other published results of similar materials. It should be stated that an

accurate flux of Rn emanating from both Wisconsin Red Granite and the concrete slab used have never been tested directly. This studies measurements can only be compared to similar materials measured in other studies. Further testing should be done to ensure that the RAD7 counts accurately and consistently measure the correct Rn concentration inside the flux chamber.

Similar average Rn fluxes are obtained using small, medium and large flux chambers, but measurement variability is systematically greater for the smaller chambers. The extra small, small, medium, and large chambers had 45.4%, 32.5%, 37.8%, and 29.6% variability from the average flux for the Wisconsin Red Granite. The same chambers had 32.8%, 31.6%, 10.8%, and 11.2% variability for the concrete slab tested. For field measurements, where structure within the Rn barrier will be more variable, these trends are expected to be exaggerated. Large flux chambers (e.g., > 2.0 m^2) are recommended to limit measurement variability.

Radon concentrations measured using AC canisters are approximately 30-40% lower than concentrations measured using the RAD7. The AC to RAD7 Rn concentration averaged 0.58 and the difference appears systematic. When J_o, A, T and RH were varied, no variable showed statistically convincing evidence that they were affecting the AC canister's ability to measure radon. Most likely, the error is related to a kinetic delay that prevents passive sorption of Rn from accurately measuring an increasing Rn concentration inside the flux chamber or the correction factors developed for a relatively static residential basement are not appropriate for these types of flux chambers where there is a Radon buildup curve.

1.7. REFERENCES

ASTM D5093 (2015) Standard Test Method for Field Measurment of Infiltration Rate Using Double Ring Infiltrometer with Sealed-Inner Double Ring. *Annual Book of ASTM Standards,* ASTM International, West Conshohocken, PA.

Albrecht, B. and Benson, C. (2001), Effect of Desiccation on Compacted Natural Clays. *J. Geotechnical and Geoenvironmental Engineering*, 127(1), 67-75.

Albright, W., Benson, C., Gee, G., Abichou, T., McDonald, E., Tyler, S., and Rock, S. (2006), Field Performance of a Compacted Clay Landfill Final Cover at a Humid Site. *J. Geotechnical and Geoenvironmental Engineering*, 132 (11) 1393-1403.

Albright, W., Benson, C., Gee, G., Abichou, T., Tyler, S., Rock, S. (2006), Field Performance of Three Compacted Clay Landfill Covers, *Vadose Zone J*., 5(6), 1157-1171.

Benson, C. (1991), Predicting Excursions Beyond Regulatory Thresholds of Hydraulic Conductivity Using Quality Control Measurements, *Proc. of the First Canadian Conference on Environmental Geotechnics*, Montreal, May 14-17, 447-454.

Benson, C., Abichou, T., Olson, M., and Bosscher, P. (1995), Winter Effects on the Hydraulic Conductivity of Compacted Clay, *J. Geotech. Eng.,* 121(1), 69-79.

Benson, C., Albright, W., Fratta, D., Tinjum, J., Kucukkirca, E., Lee, S., Scalia, J., Schlicht, P., Wang, X. (2011), Engineered Covers for Waste Containment: Changes in Engineering Properties and Implications for Long-Term Performance Assessment, NUREG/CR-7028, Office of Research, U.S. Nuclear Regulatory Commission, Washington, DC.

Benson, C. and Othman, M. (1993), Hydraulic Conductivity of Compacted Clay Frozen and Thawed In Situ, *J. Geotech. Eng.,* 119(2), 276-294.

Benson, C., Sawangsuriya, A., Trzebiatowski, B., and Albright, W. (2007), Post-Construction Changes in the Hydraulic Properties of Water Balance Cover Soils, *J. Geotech. and Geoenvironmental Eng.,* 133(4), 349-359.

Chao, C. and Tung, T. (1999), Radon Emanation of Building Material-Impact of Back Diffusion and Difference Between One-Dimensional and Three-Dimensional Tests. *Health Physics* 76 (6) 675-681.

Chao, C., Tung, T., Chan, D. and Burnett, J. (1997), Determination of Radon Emanation and Back Diffusion Characteristics of Building Materials in Small Chamber Tests. *Building and Environment*, 32(4), 355-362.

Center for Nuclear Waste Regulatory Analysis (2012), *Analysis of Mill Tailings Cover Performance*. Prepared for Nuclear Regulatory Commission, by the Center for Nuclear Waste Regulatory Analysis, Rockville, MD

Countess, R.J. (1976), Radon Flux Measurment with Charcoal Canister. *Health Physics*, 31, 455-456

Daoud and Renken (1999), Laboratory Measurments of the Radon Gas Diffusion Coefficeint for a Fractured Concrete Sample and Radon Gas Barrier Systems. *International Radon Symposium*, Report 14.

DOE (1989), Technical Approach Document. Albuquerque, NM: Prepared for The Uranium Mill Tailings Remedial Action Program. US Department of Energy, Washington, DC.

Ferry, C., Richon, P., Beneito, A., and Robe, M.C. (2002) Evaluation of the effect of a cover layer on radon exhalation from uranium mill tailings: transient radon flux analysis. *Journal of Enviornmental Radioactivity*. 63, 49-64.

Gervino, G., Bonetti, R., Cigolini, C., Marino, C., Prati, D. and Pruiti, L. (2004), Environmental Radon Monitoring: Comparing Drawbacks and Performance of Charcoal Canisters, Alpha Track and E-PERM detectors. *Nuclear Instruments and Methods in Physics Research*, 518, 452-455.

Hartley, J.N. and Freeman H.D. (1985) Radon Flux Measurements on Gardinier and Royster Phosphogypsum Piles Near Tampa and Mulberry, Florida. Prepared for US Environmental Protection Agency. DE-ACO6-76RLO 1830.

Othman, M., Benson, C., Chamberlain, E., and Zimmie, T. (1994), Laboratory Testing to Evaluate Changes in Hydraulic Conductivity Caused by Freeze-Thaw: State-of-the-Art, *Hydraulic Conductivity and Waste Containment Transport in Soils, STP 1142*, ASTM, S. Trautwein and D. Daniel, eds., 227-254.

Oak Ridge Associated Universities (ORAU) (2014), Pilot Study Report for Radon Exhalation Measurements. Prepared for US Nuclear Regulatory Commission. DCN: 2052-TR-01-0(RFTA 11-016)

Suter, G. (1993), Compacted Soil Barriers at Abandoned Landfill Sites are Likely to fail in the Long Term. *Journal of Environmental Quality*, 22 (2), 217-226.

Tuccimei P., Moroni, M. and Norcia, D. (2006), Simultaneous Determination of ^{222}Rn and ^{220}Rn Exhalation Rates from Building Materials Used in Central Italy with Accumulation Chambers and Continuous Solid State Alpha Detectors: Influence of Particle Size, Humidity and Precursors Concentration. *Applied Radiation and Isotopes*, 64, 254-263.

Ujic, P., Celikovic, I., Kandic, A. and Zunic Z. (2008) Standardization and Difficulties of Thoron Exhalation Rate Measurements Using an Accumulation Chamber. *Radiation Measurements*, 43, 1396-1401.

UMTRCA (2013), Uranium Mill Tailings Radiation Control Act Sites. Office of Legacy Management, US Department of Energy, Washington, DC.

Vanmarcke, E. (1983), *Random Fields–Analysis and Synthesis*, MIT Press, Cambridge, MA.

Vargas, A. and Ortega, X. (2007) Influence of Environmental Changes on Integrating Radon Detectors: Results of and Intercomparsion Exercise. *Radiation Protection Dosimetry*, 123 (4) 529-536.

Waugh, W., Benson, C., and Albright, W. (2015), Evaluation of Soil Manipulation Methods to Transform Engineered Earthen Covers for Long-Term Waste Containment" *J. Environmental Quality*, doi:10.2134/jeq2015.01.0001.

1.8. TABLES

Table 1.1 Summary of all concrete slab tests. *Jo* averaged 4.89 Bq/m^2-h over all tests. The back diffusion coefficeint (*D*) cannont be averaged across all tests because not all tests were run to equilibrium.

Chamber	Flux Area	*Jo* (Av)	*Jo* (Best Fit)	*Jo* (Me)	Me
	[m^2]	(Bq/m^2-h)	(Bq/m^2-h)	(Bq/m^2-h)	(Bq/m^3-h)
Extra Small	0.018	3.0	2.5	3.5	23.2
		4.1	2.9	5.2	48.1
		2.7	2.2	3.1	28.6
		2.5	2.1	2.8	26.3
		2.5	2.2	2.7	25.4
		5.8	5.9	5.7	52.6
		5.4	4.0	6.8	63.4
Small	0.071	8.1	7.9	8.3	54.6
		3.7	3.6	3.7	24.0
		4.1	3.7	4.4	28.9
		5.8	5.2	6.3	41.6
		6.5	4.2	8.8	57.6
		6.4	8.7	4.1	26.9
Medium	0.590	6.3	5.8	6.8	19.1
		4.3	4.5	4.0	11.6
		4.9	4.4	5.5	15.8
		5.0	4.8	5.2	14.9
		5.4	4.9	5.9	16.9
		5.4	4.4	6.5	18.8
		4.1	4.2	4.1	11.7
		4.6	4.5	4.7	13.7
Large	2.323	6.5	6.4	6.5	42.7
		5.3	4.9	5.7	37.3
		4.7	5.1	4.2	33.9
		5.7	5.0	6.4	42.5
		4.4	4.3	4.5	29.5
		4.9	4.6	5.2	34.5
		5.2	5.2	5.2	34.2

Table 1.2 Summary of all Wisconsin Red Granite tests. *Jo* averaged 3.23 Bq/m^2-h over all tests. The back diffusion coefficeint (*D*) cannont be averaged across all tests because not all tests were run to equilibrium.

Chamber	Area	Eo (Av)	Eo (Best Fit)	Eo (Me)	Me
	[m2]	(Bq/m^2-h)	(Bq/m^2-h)	(Bq/m^2-h)	(Bq/m^3-h)
Extra Small	0.018	7.1	6.6	7.5	69.6
		2.4	2.0	2.7	25.1
		3.4	3.3	3.4	31.5
		6.2	6.6	5.7	53.2
		2.5	2.1	2.9	26.8
		2.7	2.7	2.6	23.8
Small	0.071	6.4	4.8	8.0	52.6
		3.5	3.6	3.3	22.9
		4.4	3.7	5.1	33.4
		1.7	1.8	1.5	9.7
		3.9	3.2	4.5	29.4
		2.9	2.7	3.1	18.1
		1.8	1.2	2.3	14.8
		5.3	4.0	6.5	42.6
		2.4	2.2	2.6	16.8
		2.8	1.7	3.9	25.6
		3.4	2.0	4.7	31.1
Medium	0.590	2.5	2.0	3.0	8.7
		1.8	1.7	1.8	5.3
		2.4	2.1	2.6	7.5
Large	2.323	4.6	4.3	4.8	31.6
		4.8	4.7	4.8	31.6
		4.5	4.4	4.5	29.7
		2.5	2.3	2.6	16.9
		2.0	2.2	1.8	11.8
		2.6	2.2	2.9	19.3
		2.0	2.2	1.8	11.7
		4.3	4.7	3.8	25.0
		2.9	2.6	3.1	20.2
		2.4	2.4	2.4	15.9
		2.8	2.3	3.2	21.0
		2.5	2.5	2.5	16.6

Table 1.3 Rn Fluxes from granite, tuff, and volcanic ashes.

Source		Rn Flux, *J*		Diffusion Coefficient, *D*
		(Bq/m2-h)	(pCi/m2-h)	(1/h)
This Study	Wisconsin Red Granite	3.23	0.030	6.27E-03
	Concrete Slab	4.89	0.037	1.66E-03
Chao et al. (1997)	Granite 1	13.42	0.101	7.22E-04
	Granite 1, repeat	13.45	0.101	6.55E-04
	Granite 2	0.58	0.004	5.40E-03
	Concrete Slab	8.69	0.065	6.18E-03
Chao and Tung (1999)	Granite - Highest	13.44	0.101	-
	Granite - Lowest	0.38	0.003	-
	Granite - Average	1.82	0.014	-
Tuccimei et al. (2006)	Various Tuffs	5.47 - 1.12	0.041 - 0.008	-
	Rosso Veronese	0.04	0.0003	-
	Various Volcanic Ashes	37.08 - .086	0.278 - 0.007	-

Notes: D for Wisconsin Red Granite and the concrete slab are obtained from a test that ran to equilibrium. Hyphen indicates data not available.

Table 0.1. Summary of all AC-RAD7 direct comparison tests.

	Area	Jo	Test Duration	Rad7 Value	AC Value	Rn Ratio
	[m2]	[Bq/m2-h]	[h]	[Bq/m3]	[Bq/m3]	[RnC AC/RnC RAD7]
Area Varied	0.018	6.0	48	55	44	0.81
	0.071	4.2	48	175	129	0.74
	0.071	4.2	48	161	133	0.83
	0.590	6.9	48	409	252	0.62
"Baseline"	2.323	6.2	51	1260	821	0.65
	2.323	6.5	45	1060	585	0.55
	2.323	6.0	48	1100	666	0.61
	2.323	6.2	46	1200	636	0.53
	2.323	5.6	47	1040	581	0.56
Flux Varied	2.323	0.5	48	156	111	0.71
	2.323	1.8	48	281	167	0.59
	2.323	1.8	48	279	178	0.64
"Baseline"	2.323	6.2	51	1260	821	0.65
	2.323	6.5	45	1060	585	0.55
	2.323	6.0	48	1100	666	0.61
	2.323	6.2	46	1200	636	0.53
	2.323	5.6	47	1040	581	0.56
Time Varied	2.323	5.6	12	427	238	0.56
	2.323	6.6	24	686	327	0.48
"Baseline"	2.323	6.2	51	1260	821	0.65
	2.323	6.5	45	1060	585	0.55
	2.323	6.0	48	1100	666	0.61
	2.323	6.2	46	1200	636	0.53
	2.323	5.6	47	1040	581	0.56
Time Varied	2.323	6.6	72	1100	662	0.60
	2.323	6.0	96	1320	792	0.60
Time After Equillibrium Varied	0.071	6.0	96	224	122	0.55
	0.071	6.0	120	263	170	0.65
	0.071	6.0	144	277	200	0.72
	0.071	6.0	168	226	152	0.67

1.9. FIGURES

Figure 1.1 Photo of a 0.071 m^2 Rn flux chamber passively accumulating radon with activated carbon. This is the standard practice currently used by UMTRCA guidelines.

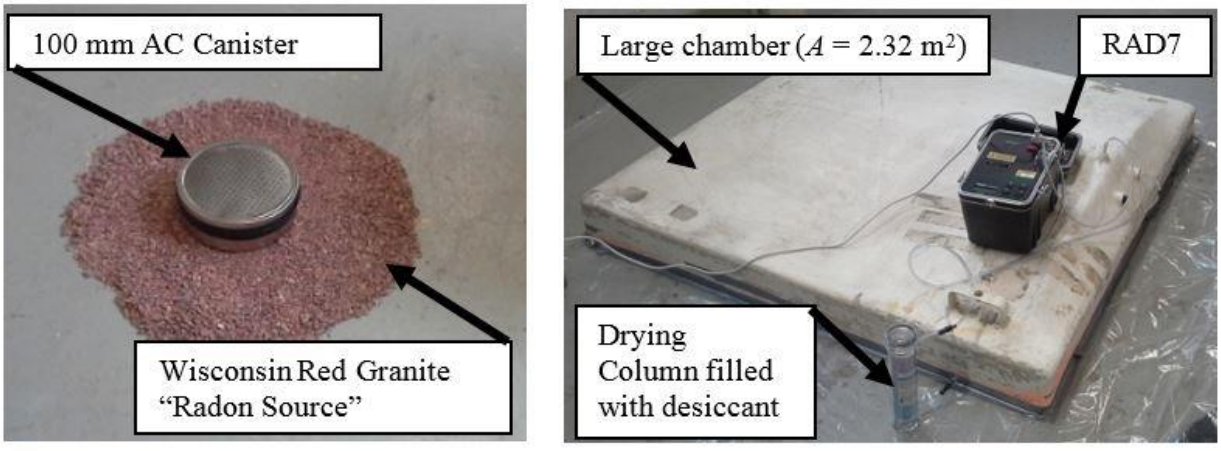

Figure 1.2 (Left) AC canister placed on granite aggregate Rn source; (right) RAD7 sampling the atmosphere within a large chamber overlying a layer of granite on top of the plastic sheeting.

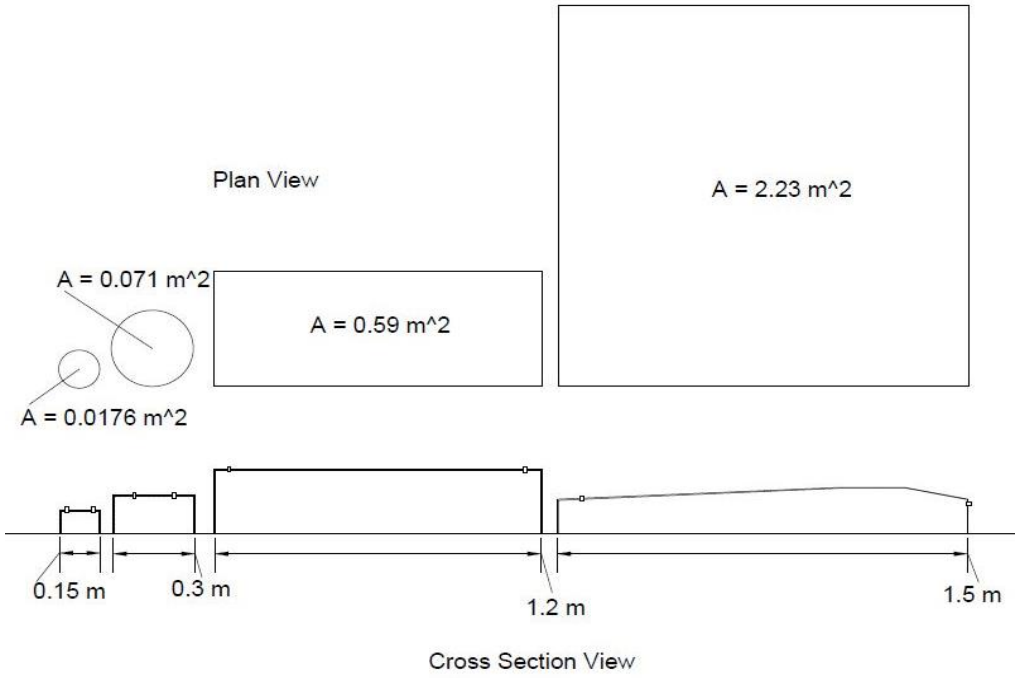

Figure 1.3 Scaled image of the dimensions of each flux chamber.

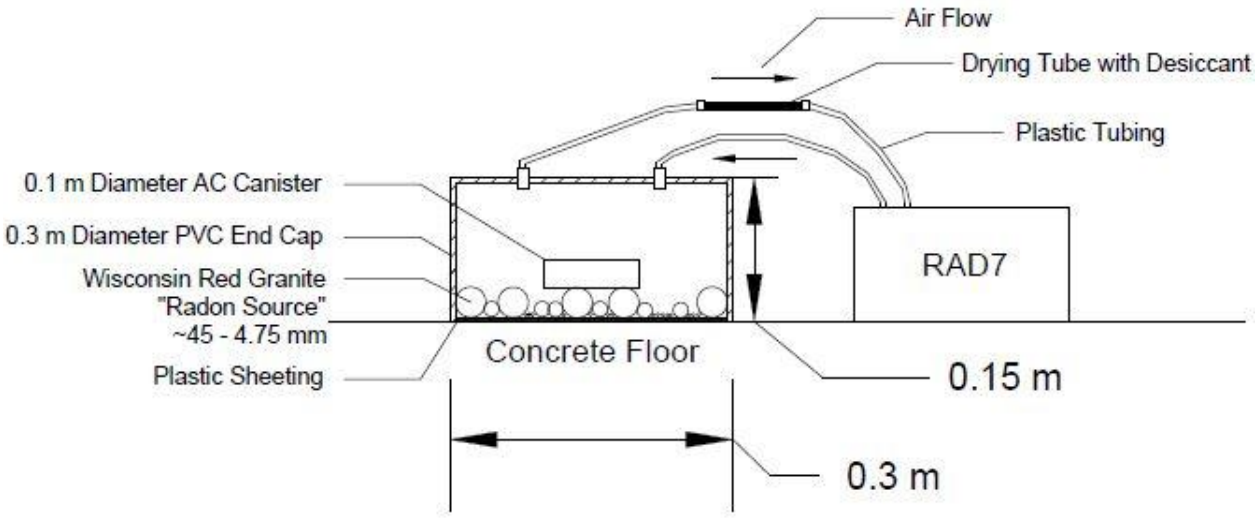

Figure 1.4 Experimental set up for the small flux chamber.

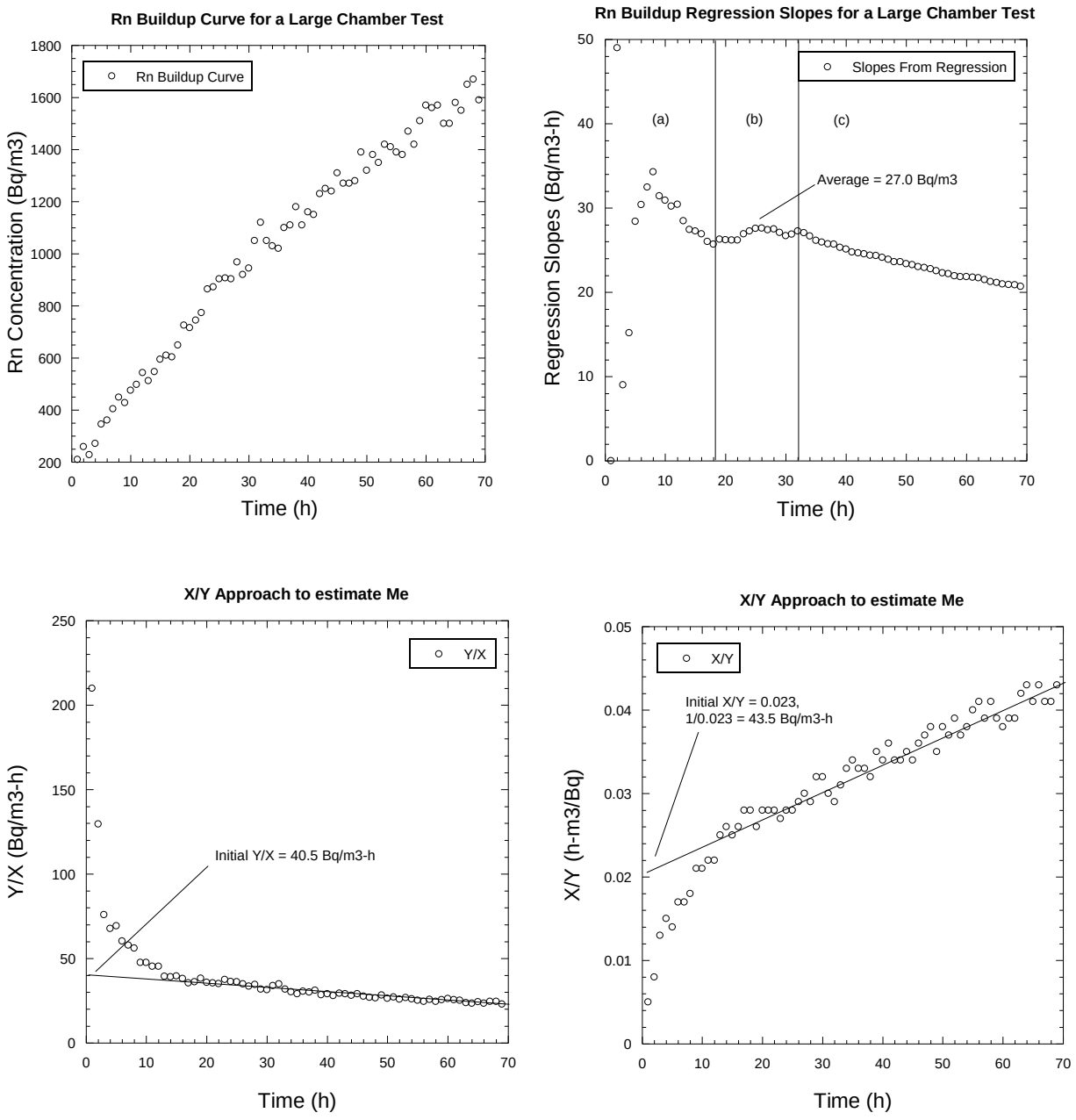

Figure 1.5 A Rn buildup curve and three approaches to determine M_e.

Figure 1.6 Two AC canisters placed in the chamber pre exposing them to RH. This chamber has RH of 16% due to the salt bath.

Figure 1.7 Experimental set up of AC canisters pre exposed to different RH ready to be exposed to Rn in the large chamber.

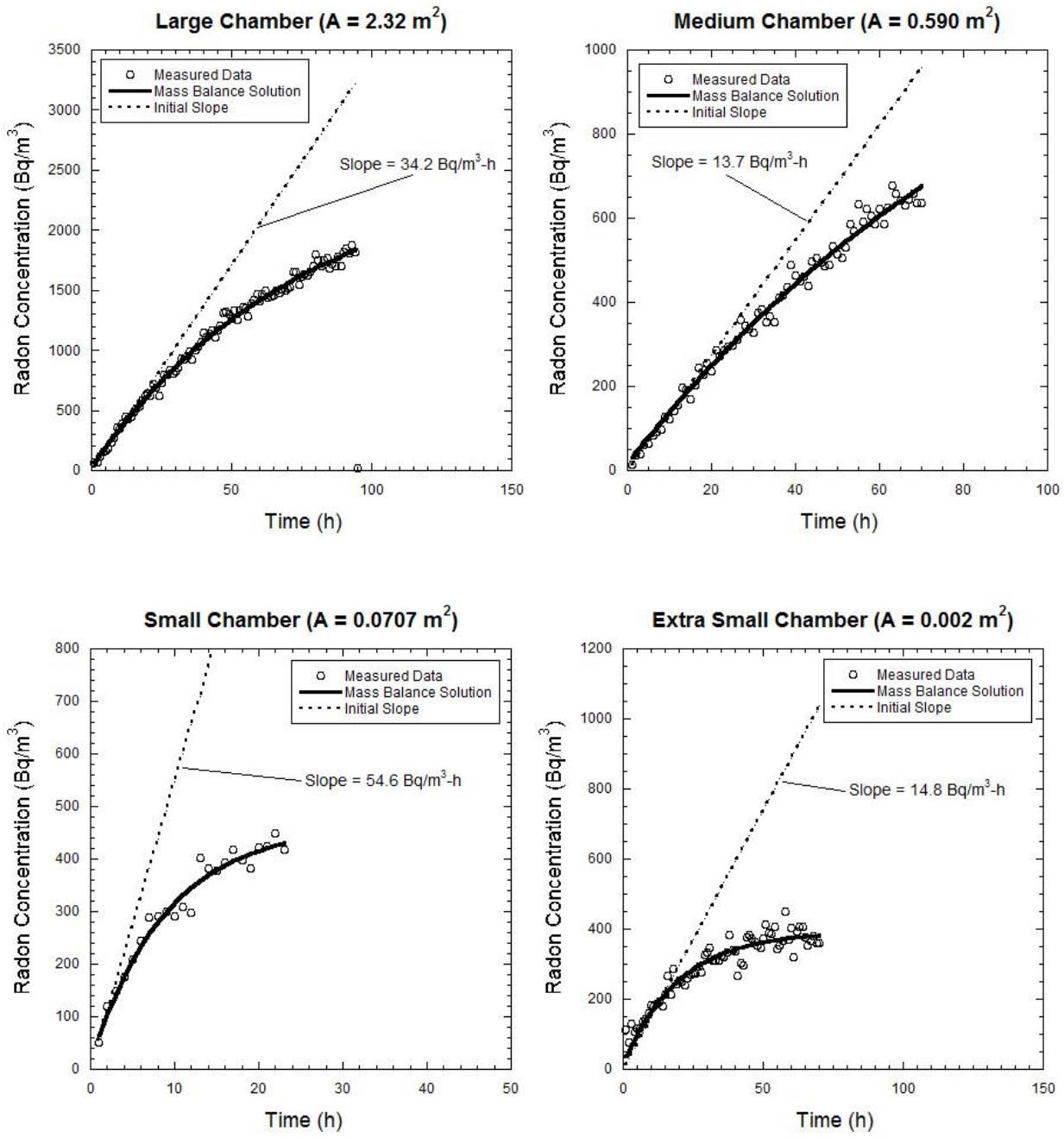

Figure 1.8 Radon concentration buildup curves for the concrete slab. One test representative of each chamber is presented.

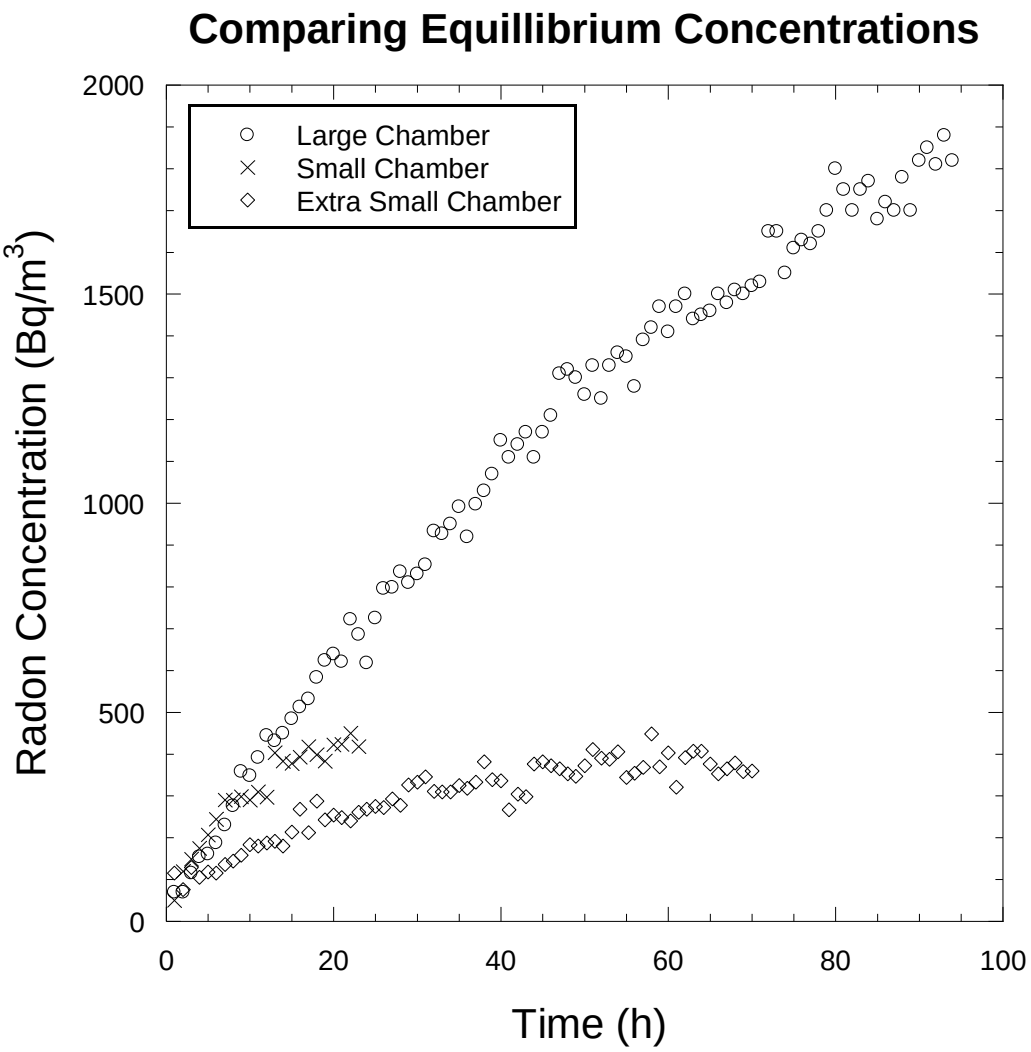

Figure 1.9 If the volume to area ratio is similar between each chamber, the equilibrium concentration increases as the flux area increases.

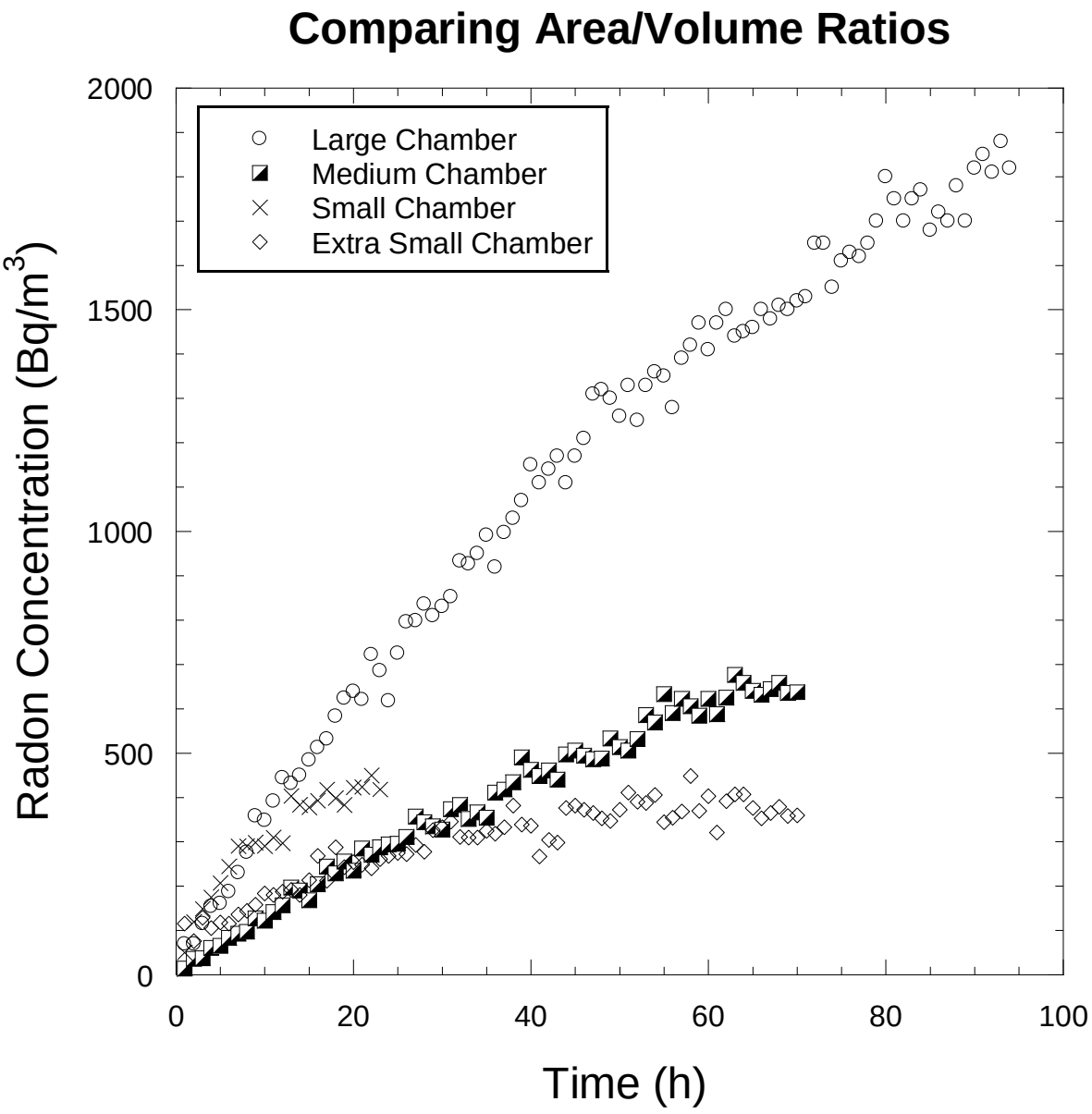

Figure 1.10 The medium buildup curve (half-filled data points) builds slower than the other three chambers that all have a smaller volume to area ratios.

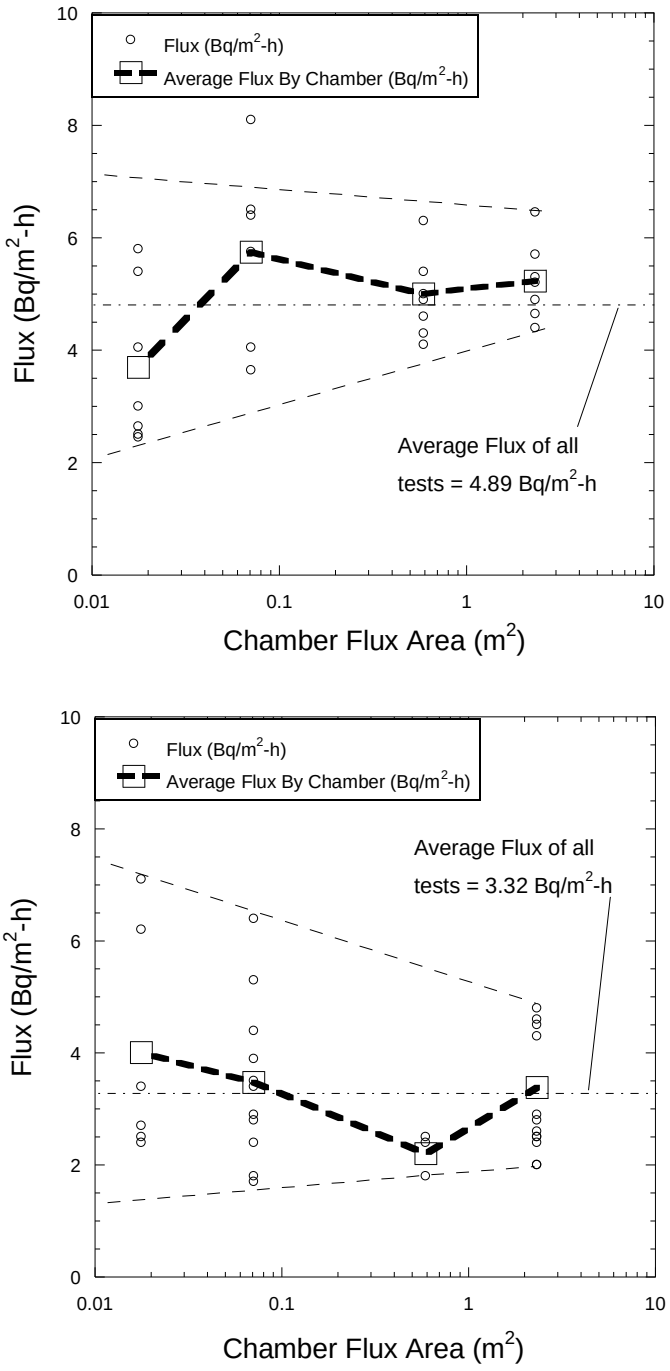

Figure 1.11 Rn flux tests as a function of flux area for both concrete (top) and granite (bottom). The average flux for all tests is the flat dashed line. The average flux for each chamber size is the large open square.

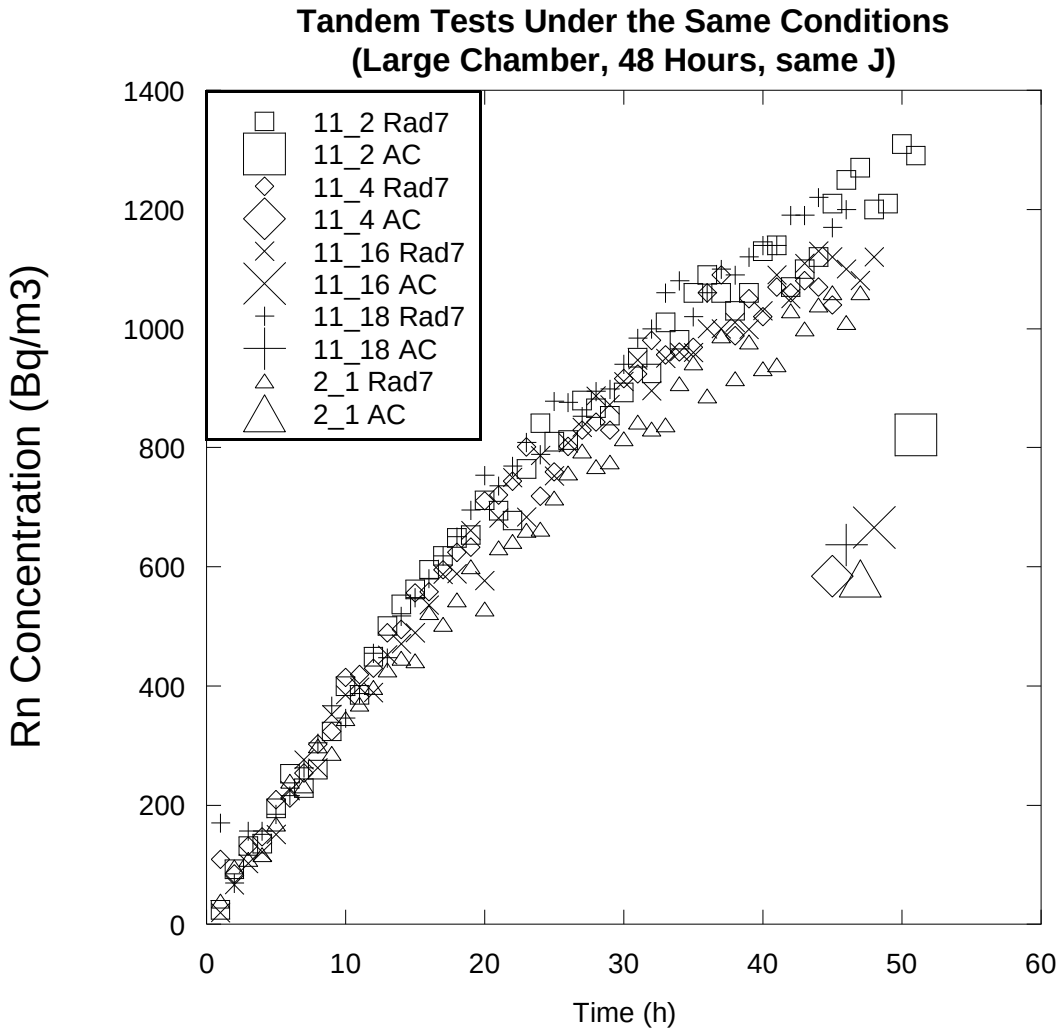

Figure 1.12 Direct comparison of measured Radon between AC and RAD7 observed data. AC to RAD7 Rn concentration averages 0.58.

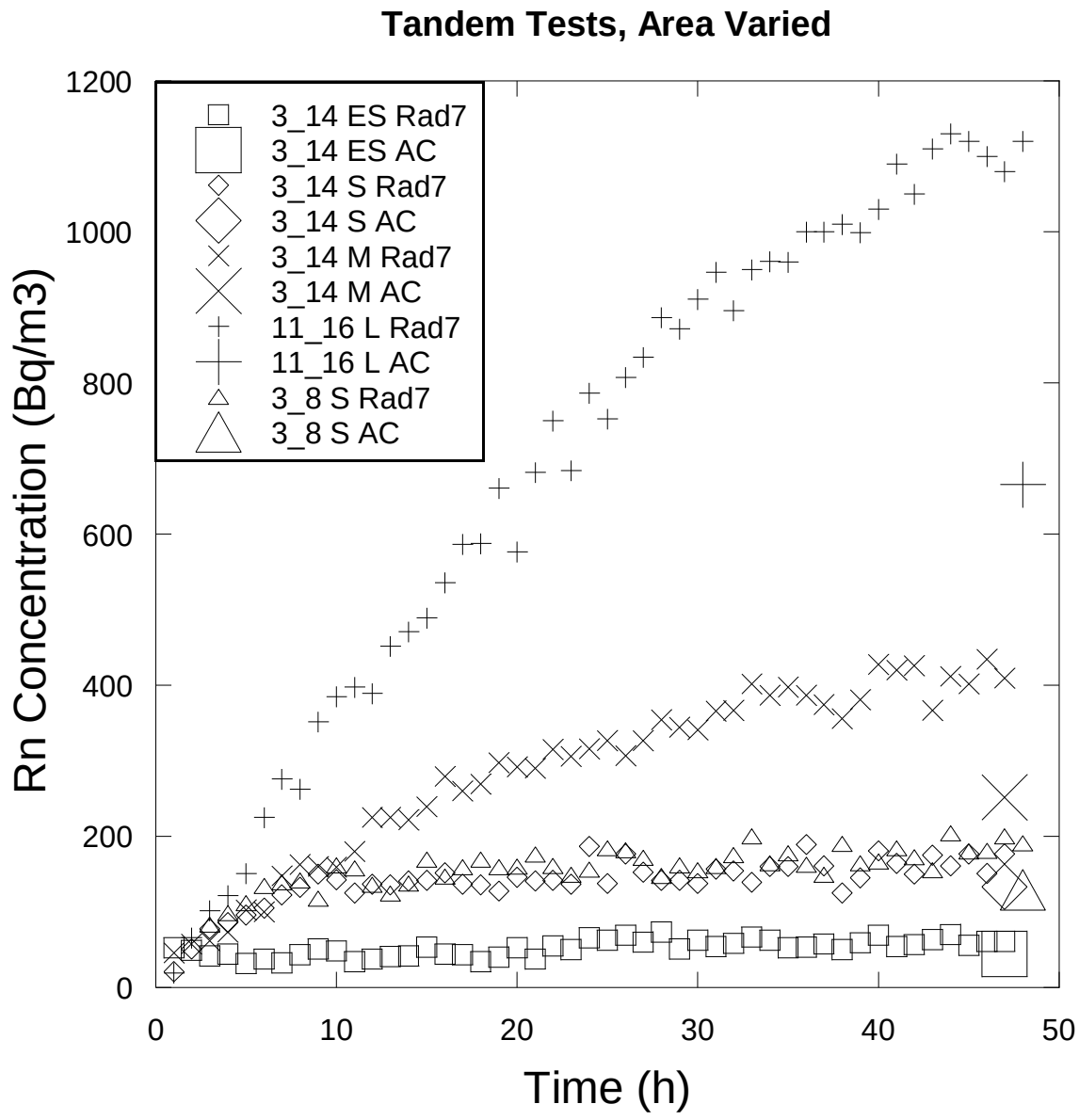

Figure 1.13 Direct comparison of AC and RAD7 measurements as flux area is varied.

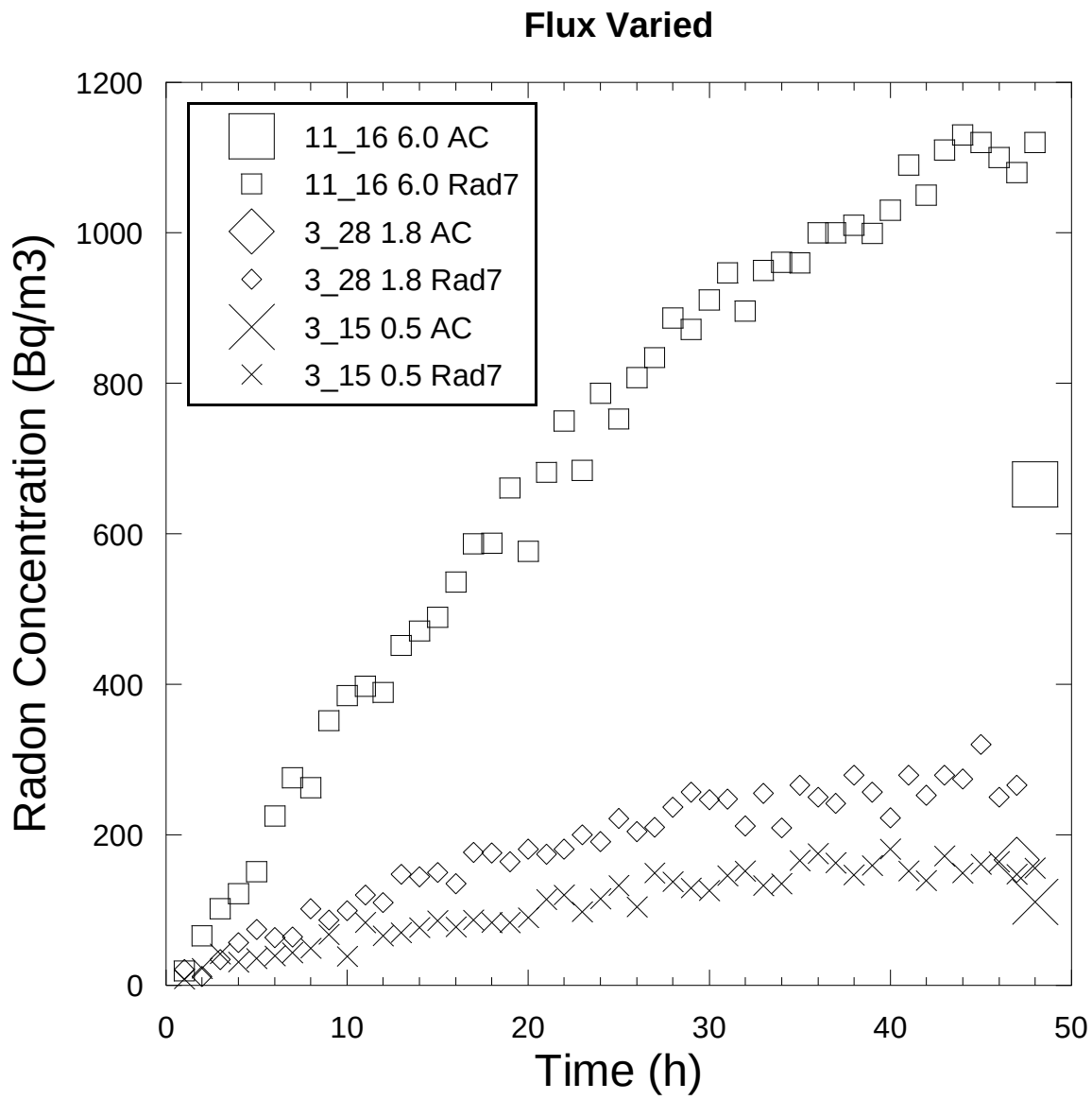

Figure 1.14 Direct comparison of AC and RAD7 measurements as flux is varied. Flux was varied by changing the mass/area ratio.

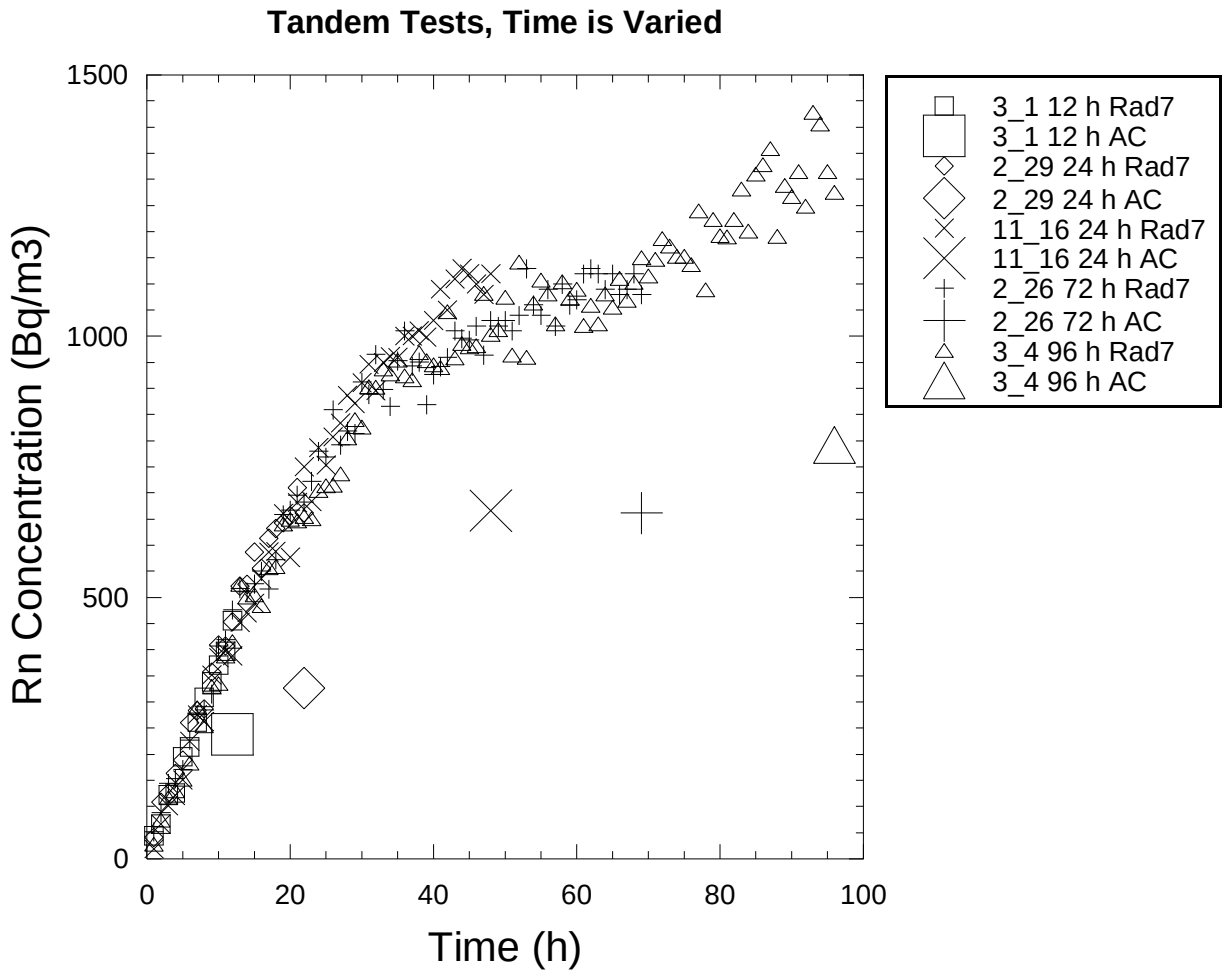

Figure 1.15 Direct comparison of AC and RAD7 measurements as exposure time is varied.

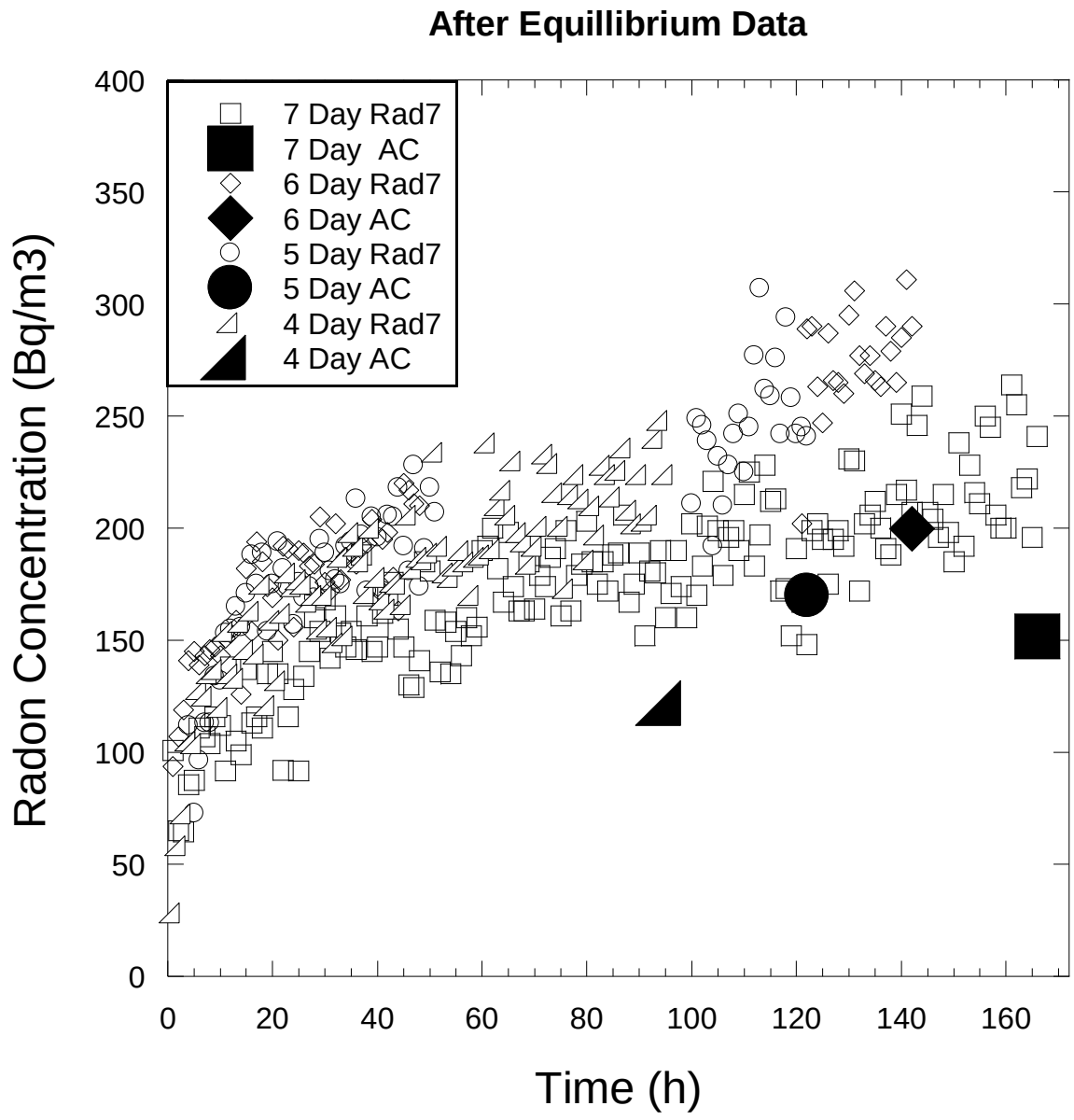

Figure 1.16 Direct comparison of AC and RAD7 measurements as time after equilibrium was varied. Tests were intended to be run in increasing intervals past equilibrium of Radon concentration inside the chamber. Unintended, the 5 d and 6 d tests show an uptick in Radon near the end of the test.

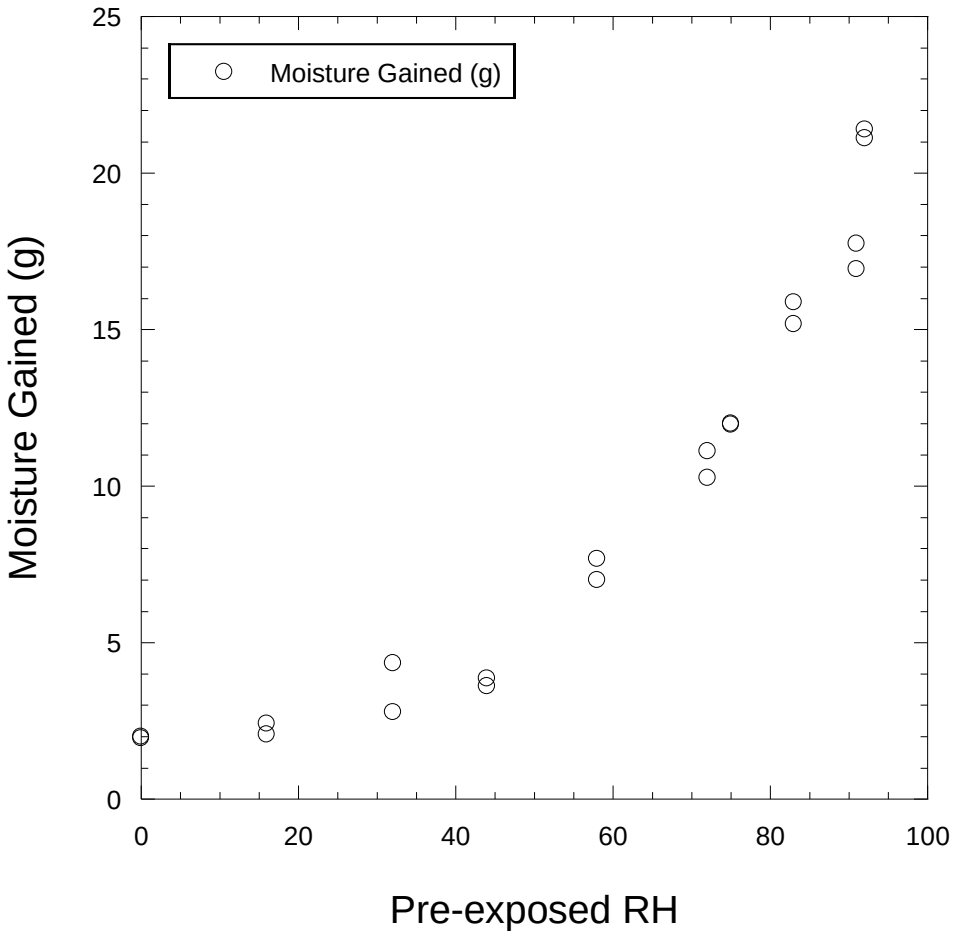

Figure 1.17 Moisture gained on the AC canister increased as the pre exposure Relative Humidity increased

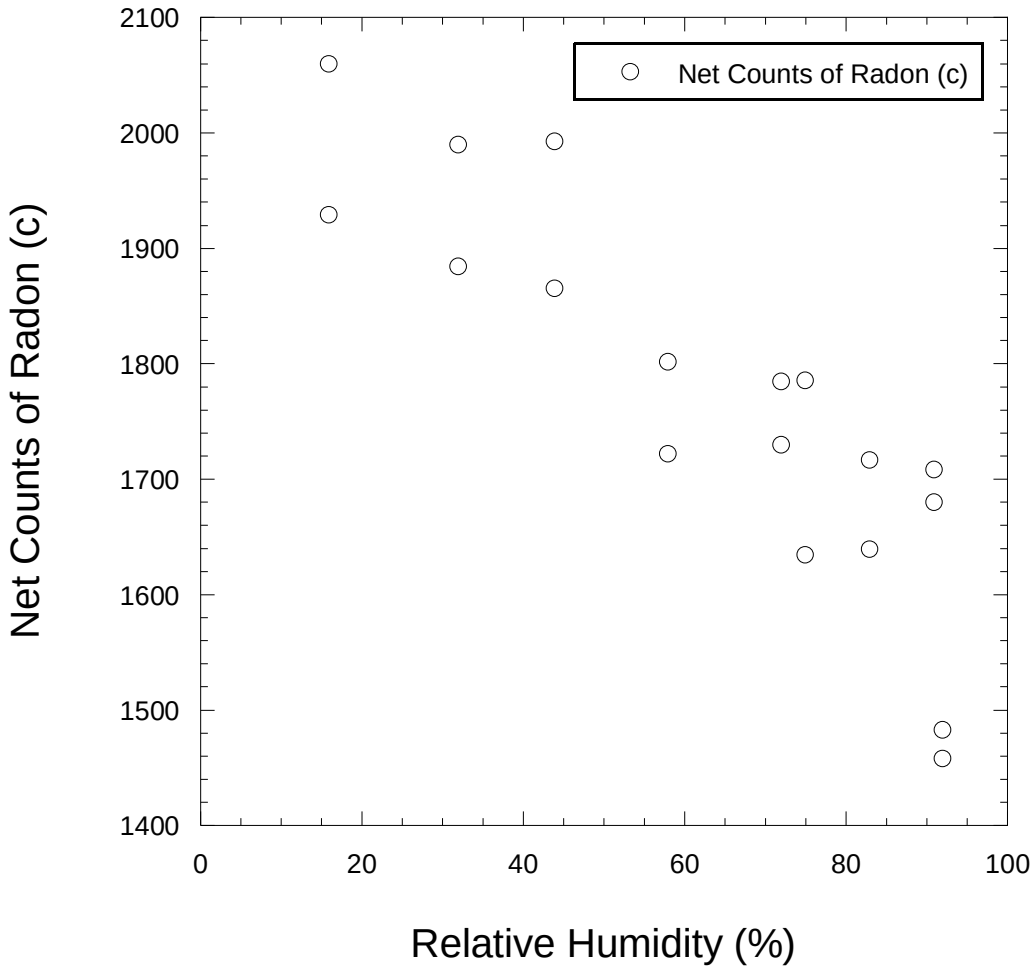

Figure 1.18 Passive sorption of Radon decreased as it was pre exposed to higher levels of Relative Humidity.

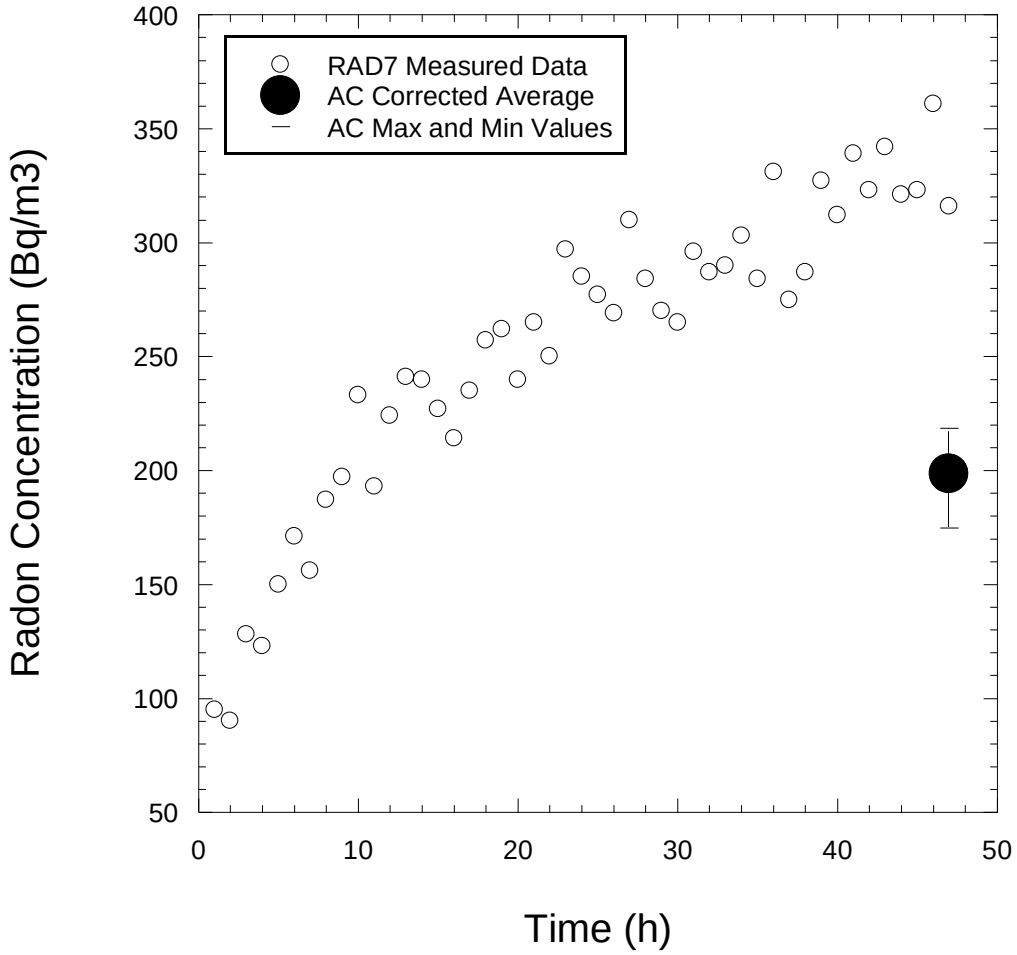

Figure 1.19 RAD7 buildup curve from RH variation test. The average corrected AC value was 198.5 Bq/m^3, the filled circle. The error bars are the maximum and minimum corrected values from RTCA's analysis, 218.5 and 174.7 Bq/m^3.

Chapter 2

EFFECTS OF WET-DRY CYCLING ON RADON DIFFUSION COEFFICIENTS FOR COMPACTED CLAYS

2.1. ABSTRACT

Effective Radon diffusion coefficients (D_{Rn}) were measured for compacted clay specimens subjected to wet-dry cycles to quantify the effects of soil structure development on gaseous Radon diffusion coefficient. A new laboratory apparatus was developed by modifying a flexible-wall permeameter cell to accommodate circulation and measurement of Radon gas on the top and bottom boundaries of the specimen. Six clays with varying plasticity index (PI) values (9 < PI < 26) were compacted at optimum moisture and density conditions to replicate initial placement conditions common of compacted clay cover systems. All soils tested have been used for actual cover systems, and thus are considered representative of typical barrier materials. Compacted clay specimens with dimensions of ~50 mm in thickness and 100 mm in diameter were placed inside a 100 mm (4”) diameter permeameter cell. Two solid state alpha detectors (RAD7 from Durridge Company Inc.) were used to continuously measure radon concentrations in two chambers forming the top and bottom specimen boundaries. The bottom boundary was circulated with a fixed, source concentration of Radon created by circulating air through a column filled with granite aggregate. The top boundary was used to monitor buildup of Radon with time as the gas form the source at the bottom boundary diffused through the specimen. About 24 h was needed to determine a radon flux and calculate corresponding diffusion coefficient. Samples could be tested multiple times to produce replicate data by periodically purging the top boundary and reinitializing subsequent build up curves.

Effective radon diffusion coefficients were measured after initial compaction of specimens at optimum water content, after the specimens were fully saturated, and after the specimens were dried in an oven at 50 ˚C. Specimens were subjected to four wet-dry cycles between full saturation and drying at 50 ˚C. Diffusion coefficients were measured at each step in the cycle. Measured effective diffusion coefficients for the six clays ranged from 3.98E-7 m^2/s to 1.24E-9 m^2/s. Diffusion coefficients at full saturation were systematically about 0.9 to 0.3 orders of magnitude less than for oven dried conditions. The difference between the oven dried and fully saturated samples ranged from 3.28E-7 m^2/s and 6.76E-8 m^2/s. For the presented data, D_{Rn} for all six clays do not show any clear trends with wet-dry cycling. In some cases, D_{Rn} decreased significantly after the first cycle and continued to gradually trend downward with increasing wet-dry cycles. Trends for the clays of higher plasticity (Denver and KF2, PI = 26) indicated that the dry D_{Rn} and saturated D_{Rn} increased and decreased through multiple cycles. For clays of lower plasticity (Lodgement and Phoenix, PI = 11 and 9 respectively), trends in D_{Rn} were essentially constant regardless of the number of wet-dry cycles. Despite the lack of clear trends, the methodology was found to produce D_{Rn} measurements that are in good agreement with other studies reporting D_{Rn} or other gaseous diffusion coefficients (O_2 and CO_2) through compacted clay cover materials.

2.2. BACKGROND

In 1978, the Uranium Mill Tailings Radiation Control Act (UMTRCA) was passed to manage low-level radioactive waste tailings. UMTRCA disposal cells are located throughout much of the western US and are exposed to varying environmental conditions. The UMTRCA act designated the lifespan of each disposal cell to be 1,000 years. While each UMTRCA site is different, the primary component of the barrier system is a low-permeability layer, called the Radon Barrier (Figure 2.1). A supplementary protection layer is designed to limit environmental exposure that could lead to degradation of the primary Radon barrier. In some cases an additional bedding layer is present below rip rap or topsoil to support vegetation at the surface.

The Rn barrier is compacted to limit transport of water and gas. Water can leach into the tailings and seep into the ground water creating a human health risk. However this study will focus on the transport of a gas, primarily radon. Radon is an airborne, alpha decay contaminant and the constructed Rn barrier creates a diffusion barrier for radon to pass through.

The radon diffusion coefficient (D_{Rn}) is the primary value in determining the Rn barrier thickness. D_{Rn} also quantifies how much radon diffuses through the barrier and out through the top into the environment (radon flux). This radon flux was measured once the Rn barrier was completed to comply with the maximum allowable radon flux stipulated by UMTRCA (2664 Bq/m^2-h or 20 pCi/m^2-s). However, the Center for Nuclear Waste Regulatory Analyses (2012) conducted measurements of radon fluxes many years after at select sites and found that Rn flux varied from 26,640 Bq/m^2-h (200 pCi/m^2-s) and as low as 39.9 Bq/m^2-h (0.3 pCi/m^2-s). Even though diffusion is heavily controlled by the saturation of the Rn Barrier and this varies throughout the year, there is the potential that pedogenisis (structural development in response to soil formation processes) is degrading the Rn barrier, especially over long periods of time (20+ years).

At these time scales, Suter (1993), Benson et al. (2007), and Waugh et. al (2015) have all observed degradation of compacted clay cover systems. Freeze-thaw cycles, wet-dry cycles, and bio-intrusion are all potential sources that could compromise the Rn Barrier. These processes are known to alter the hydraulic conductivity of cover systems by several orders of magnitude (Benson and Othman 1993, Othman et al. 1994, Benson et al. 1995).

Because D_{Rn} is a critical value in the initial design and it dictates radon flux through the top of the cover, it has been measured and analyzed through different testing contexts, comparing field measurements to lab measurements, comparing steady state vs transient calculation approaches and comparing how D_{Rn} is different through different borrow materials selected for the Rn barrier (Kalkwarf et al 1982 and Lepel 1982). Other mine tailings sites also have data on diffusion coefficients of other gases that can be adapted to measuring radon diffusion (Elberling et al. 1994 and Aachib et al. 2004). Ideally, these approaches can be used to correlate lab and in situ measurements and also understand how the Rn barrier is changing due to environmental factors.

There have been many approaches to model gas diffusion coefficients through soil media. Elberling et al. (1994) sampled gas concentrations along the profile of the soil column. However this method requires the sampling points be separated enough to not affect the diffusion process and requires multiple sensors. Alternative approaches use two sensors to measure gas concentrations on either side of the soil medium (Lepel et al. 1983; Yanful 1993; and Jiranek and Hulka 2000). Aachib et al. (2004) flooded one side of the soil medium with O_2 and continually purged the other. To begin the test, both chambers on the sides of the soil were sealed and the concentrations were measured continuously until they reached equilibrium. This method and solution are applicable for gas species that remain chemically inert with the soil sample. Because radon has a short half-life (3.8 days), decay must be accounted into the

solution and can create complications for transient solutions to track the mass of radon diffusion from one chamber to the other.

Kalkwarf et al. (1982) compared transient and steady state solutions for Rn diffusion. Through steady state analysis, two of the four boundary conditions are needed to arrive at a solution; (a) the initial Rn flux from the bare radon source, (b) the Rn flux from the exit end of the sample column, (c) the Rn concentration at the entrance of the soils sample, or (d) the Rn concentration at the exit of the column. These four variables are easy to monitor and control with a continuous radon monitor (RAD7).

2.3. METHODS AND MATERIALS

2.3.1. Compacted Clays

All six clays used in this study were selected because they all have been used in compacted clay cover systems and are representative of borrow material used in its construction. The clays have been used in previous studies (Benson 1995; Albrecht and Benson 2001; Benson 1997) to quantify changes to hydraulic conductivity in cover systems. The plasticity index values are summarized in Table 2.1.

2.3.2. Electronic Radon Monitor (RAD7)

Continuous electronic radon monitors employ a solid state alpha detector to measure the alpha decay chain of Radium. The RAD7 (Durridge Company Inc.) is capable of distinguishing specific disintegrations to accurately and reliably measure radon. RAD7 devices are common in laboratory work measuring radon build up in hermetically sealed chambers (Chao et al. 1997; Tuccimei et al. 2006; Ujic et al. 2008). A common flow rate of 800 mL/min is used to cycle air from the chamber to the RAD7. Data intervals are specified by the operator, allowing calculation of buildup curves in radon concentration to calculate the initial radon flux. One hour is a common sampling interval to maximize data and minimize error. 15 minutes was occasionally used for testing when more

data points in the beginning of the buildup curve was necessary. The RAD7 provides a more robust and useful measurement technique for this application.

2.3.3. Permeameter

Permeameters commonly used for measuring hydraulic conductivity were used to measure D_{Rn}. (ASTM 5084-3). After compaction, wetting, and drying, clay pucks where placed between two plastic discs, drilled with 3 mm diameter holes spaced 7 mm apart, to provide a stable base and sufficient air flow (Figure 2.2). Polyvinyl chloride (PVC) tubes were cut into cylinders to act as chambers that were placed above and below the clay sample. They varied in length but were generally 30 mm. The base plate of the permeameter and a disc with two ports provided sampling locations for the RAD7 to measure radon. The entire column of clay and chambers was surrounded by a flexible wall membrane and sealed with O rings so that the chamber could be filled with water. 2.5 kPa water pressure was used to provide side wall pressure could ensure that there would be no side wall leakage and all radon diffused through the clay sample.

Radon sources were connected in line with the bottom chamber of the permeameter and one RAD7 to provide a constant radon concentration. Wisconsin Red Granite aggregate 40 – 4.75 mm in diameter was placed in 100 mm diameter, 500 mm length PVC tubes. Air tight fittings where drilled into the tube to provide easy connection to and from the tube. A schematic of the testing apparatus can be seen in Figure 2.3.

2.3.4. Wet-Dry Cycling Procedure

Clay samples were compacted to standard proctor at optimum water content and max dry unit weight (ASTM D698). Compacting the samples will match typical initial conditions of clay cover designs. Data for compaction came from Albrecht and Benson (2001) and from compaction curves (Figure 2.4) generated for this study. The summary of optimum water content and max dry

unit weight can be found in Table 2.2. After the sample was compacted, it was placed inside the testing apparatus and measured for D_{Rn}.

Next samples where dried in a 50 ^{o}C oven for 24 h to ensure that all water was driven out of the sample. The weight of the clay puck was tracked to make sure that all water had been evaporated. Samples were placed inside the testing apparatus again to be measured for D_{Rn}. Clay samples were saturated inside a desiccator under vacuum for 24 h. Similarly, weight was tracked to make sure sample were fully saturated. Geotextile was placed above and below the sample between the plastic discs while being saturated and a flexible membrane was sealed around the discs. This way, water could saturate through the top and bottom of the sample without disturbing the sample's shape. A tiny exposure of sample above the water ensured that air would not be trapped inside the pore space (Figure 2.5).

2.3.5. Calculating D_{Rn}

Kalkwarf et al. (1982) and Lepel et al. (1983) proposed a steady state solution for calculating the effective radon diffusion coefficients with measured boundary conditions. For the experimental testing apparatus used in this study, the initial radon flux through top surface of the soil sample and the constant radon concentration at the bottom of the soil sample were measured with RAD7 units and are used to calculate D_{Rn} values according to Eq. 1.

$$\frac{C_o}{J_o} = \frac{k*(1- e^{-2*k*x})}{\lambda*(1+ e^{-2*k*x})} = \frac{k}{\lambda} * \tanh(k * x) \quad (1)$$

Where C_o is the radon concentration (Bq/m^3) in the bottom chamber, J_o is the initial radon flux (Bq/m^2-h) after the top chamber is purged, x is the soil sample thickness, and λ is the ^{222}Rn decay constant (0.0076 1/h). D_{Rn} (m^2/s) is built into the value k from Eq. 2.

$$k = (\frac{\lambda}{D_{Rn}})^{0.5} \quad (2)$$

D_{Rn} is solved iteratively until a suitable solution is found.

Rn flux was calculated using the method discussed in Chapter 1.4.1. When time permitted, the top chamber was purged after one test so that replicate D_{Rn} data could be produced and compared.

2.4. RESULTS

2.4.1. Desiccation cracks

Figures 2.6 to 2.11 show photos taken after samples were saturated and dried. The dried samples show clear desiccation cracks. Many times after saturation, the cracks at the surface appear to fully anneal. Structural changes may be different inside the sample. Additionally, it does not appear that the extent of desiccation cracking increased as wet-dry cycles are increased. However, this conclusion is limited since it can only be assessed through visual observation.

2.4.2. Changes to D_{Rn}

Calculated D_{Rn} values are presented in Figures 2.6 to 2.11 for each of the six clays. The red data points are the fully dried measurements and the blue data are the fully saturated measurements. The plots are bounded by the diffusion coefficient of air (1e-5 m^2/s) and of water (1e-9 m^2/s) at the top and bottom of each plot (Kalkwarf et al. 1982; Hassan 2009; Ishimori et al. 2013). Since the pore space with either be comprised of air or water, measurements conducted on the clay samples should fall within this range. The black, open data point is the D_{Rn} measurement taken after compaction. Each data point in each wet-dry stage is the average D_{Rn} of all the tests run and the error bars show the maximum and minimum value measured at that stage.

The highest D_{Rn} was 3.98e-7 m^2/s and the lowest value was 1.24e-09 m^2/s. The range of data matches well with similar materials. Lepel et al. (1983) conducted laboratory measurements on an inorganic, low plasticity clay, representative of an UMTRCA clay cover to be 3.6e-7 m^2/s. Kalkwarf et al. (1982) compared steady state and transient solutions of different soils and found

that the clay used had saturations ranging from 0.1 to 0.35 had D_{Rn} values from 4.5e-6 m^2/s to 7.0e-7 m^2/s. Finally, Yanful (1993) measured O_2 diffusion coefficients through typical compacted clay covers. While the two gases are different, they should provide comparable diffusion coefficients through the same material. That study measured D_{O2} ranging from 8.0e-8 m^2/s to 6.3e-6 m^2/s for saturations ranging from 0.85 to 0.24 respectively. Because, not all the properties affecting diffusion are identical (porosity and saturation), these values cannot be compared directly to this study's findings. But they can be used to verify the experimental approach is appropriate and returning the proper magnitude expected D_{Rn} values.

It was hypothesized that there would be an upward trend in the measured values for diffusion coefficients. As soil structure developed, larger and large pore spaces would open up, allowing more radon to migrate, resulting in a higher diffusion coefficient. The measured data do not show such a trend.

In some of the higher plastic clays (Denver, Figure 2.6 and KF2, Figure 2.7) the D_{Rn} rise and fall for both the wet (0.5 orders of magnitude) and dry (0.3 orders of magnitude) cycles. New Orleans (Figure 2.8) begins with a sharp large decrease (0.8 orders of magnitude) after one cycle then shallows to decrease only slightly (0.1 orders of magnitude) as the cycles increases. Were most of the clay sample results show similar trends between the wet and dry data sets, the Atlanta clay sample (Figure 2.9) show little change in the dry D_{Rn} and significant rise and fall (as much as a full order of magnitude) in the wet D_{Rn} . It is hypothesized that more plastic clays are subjected to consolidation or compaction, decreasing pore volume and decreasing D_{Rn} leading to large swings and variations as cycles increase.

In general, the less plastic clay samples (Lodgement, Figure 2.10 and Phoenix Figure 2.11) display a fairly consistent, less than 0.2 orders of magnitude change in D_{Rn}, through four wet-dry cycles. It is expected that these clays experience less volumetric shrinkage as they are

saturated and desiccated and do not develop soil structure. Since they maintain a relatively consistent pore volume, the D_{Rn} changes little.

Unfortunately, measured thickness through the wet-dry cycles could not alone be used to characterize volumetric changes in the pore space. Clay material stuck to the plastic discs throughout different stages of the procedure, causing continual sample trimming and small amounts of material to be lost. Additionally, clays fully saturated, especially the more plastic ones, could easily be jostled or disturbed throughout various steps of the procedure, changing the soil structure or pore space unintentionally, compromising reliable D_{Rn} measurements attempting to capture changes in soil structure.

2.5. SUMMARY AND CONCLUSTIONS

Overall, there is a high degree of confidence that testing apparatus used is capable of measuring D_{Rn} reliably through soil samples. Measured Rn diffusion coefficients across all clays ranged from a maximum of 3.98e-7 m^2/s to a minimum of 1.24e-09 m^2/s. They also fall within the expected diffusion coefficients boundaries of air (1e-5 m^2/s) and water (1e-9 m^2/s). Additionally, they agree well with other measurements on other compacted clay layers, measuring diffusion of radon or similar gasses. Data cannot be compared directly because the saturation condition is different, but they can be compared to make sure observations are in the correct order of magnitude.

The adapted testing apparatus used contains a few distinct advantages to other research approaches. RAD7 and other continuous radon monitors can measure and record radon concentration data more accurately for better analysis of Rn flux through the top of the clay surface. The apparatus also makes it easy for replicate testing trials in the same wet-dry stage.

Unfortunately, there is no evidence to suggest that the wetting and drying procedure used created the intended desiccation and soil structure desired. None of the clay samples displayed an upward trend in D_{Rn} as hypothesized. However we can see that less plastic clays showed a flat trend and consistent D_{Rn} throughout wetting-drying cycles. On the other hand, more plastic clays showed more variance in D_{Rn} and even developed a shallow decrease in D_{Rn}. It is expected a combination of consolidation, compaction, or disturbance is having a negative impact on the development of soil structure being measured through steady state diffusion coefficients measurement.

2.6. REFERENCES

Aachib M., Mbonimpa. M, and Aubertin M., (2004) Measurement and Prediction of the Oxygen Diffusion Coefficient in Unsaturated Media, with Applications to Soil Covers. *Water, Air, and Soil Pollution*. 156, 163-193.

ASTM D698 Standard Test Methods for Laboratory Compaction Characteristics of Soil Using Standard Effort, *Annual Book of ASTM Standards*, ASTM International, West Conshohocken, PA.

ASTM 5084 (2003) Standard Test Methods for Measurement of Hydraulic Conductivity of Saturated Porous Materials Using a Flexible Wall Permeameters. *Annual Book of ASTM Standards*, ASTM International, West Conshohocken, PA.

Albrecht, B. and Benson, C. (2001), Effect of Desiccation on Compacted Natural Clays. *J. Geotechnical and Geoenvironmental Engineering*, 127(1), 67-75.

Center for Nuclear Waste Regulatory Analysis (2012), *Analysis of Mill Tailings Cover Performance*. Prepared for Nuclear Regulatory Commission, by the Center for Nuclear Waste Regulatory Analysis, Rockville, MD

Benson, C. (1991), Predicting Excursions Beyond Regulatory Thresholds of Hydraulic Conductivity Using Quality Control Measurements, *Proc. of the First Canadian Conference on Environmental Geotechnics*, Montreal, May 14-17, 447-454.

Benson, C. and Othman, M. (1993), Hydraulic Conductivity of Compacted Clay Frozen and Thawed In Situ, *J. Geotech. Eng.,* 119(2), 276-294.

Benson, C., Abichou, T., Olson, M., and Bosscher, P. (1995), Winter Effects on the Hydraulic Conductivity of Compacted Clay, *J. Geotech. Eng.,* 121(1), 69-79.

Benson, C.H. and Trast, J.M., (1995), Hydrauilc conductivity of thirteen compacted clays, *Clays and Clay Minerals*, 43; 669-681.

Benson, C.H., (1997) Hydraulic Characteristics of Barrier Soils for Alternative Landfill Cover Demonstration, Report Completed for RUST Environmental and Infrastructure.

Benson, C., Sawangsuriya, A., Trzebiatowski, B., and Albright, W. (2007), Post-Construction Changes in the Hydraulic Properties of Water Balance Cover Soils, *J. Geotech. and Geoenvironmental Eng.,* 133(4), 349-359.

Benson, C., Albright, W., Fratta, D., Tinjum, J., Kucukkirca, E., Lee, S., Scalia, J., Schlicht, P., Wang, X. (2011), Engineered Covers for Waste Containment: Changes in Engineering Properties and Implications for Long-Term Performance Assessment, NUREG/CR-7028, Office of Research, U.S. Nuclear Regulatory Commission, Washington, DC.

Elberling B., Nicholson R.V., Reardon E.J., and Tibble, P. (1994) Evaluation of Sulphide Oxidation Rates: a Laboratory Study Comparing Oxygen Fluxes and Rates of Oxidation Product Release. *Canadian Geotechnical Journal*. 31, 375-383.

Hassan N., et al. (2009) Radon Migration Process and Its Influence Factors; Review. *J. Health Physics*. 44 (2), 218.

Ishimori, Y., Lange K., Martin P., Mayya Y.S., and Phaneuf M., (2013) Measurement and Calculation of Radon Releases from NORM Residues. Prepared for the International Atomic Energy Agency. Technical Reports Series Number 474.

Jiranek M. and Hulka J. (2000) Radon Diffusion Coefficient in Radon-Proof Membranes – Determination and Applicability for the Design of Radon Barriers. *International Journal on Architectural Science*. 1, Number 4, 149-155.

Kalkwarf D.R, Nielson K.K., Rich D.C., and Rodgers V.C., (1983) Comparison of Radon Diffusion Coefficients Measured by Transieint-Diffusion and Steady-State Laboratory Methods. Prepared for US Nuclear Regulatory Commission. NUREG/CR-2875, NPL-4370, RAE-18-3.

Lepel E.A., Silker W.B., Thomas V.W., Kalkwarf D.R., (1984) Comparison of Field-Measured Radon Diffusion Coefficients with Laboratory-Measured Coefficients. Prepared for US Nuclear Regulatory Commission. NUREG/CR-2769, PNL-4414.

Othman, M., Benson, C., Chamberlain, E., and Zimmie, T. (1994), Laboratory Testing to Evaluate Changes in Hydraulic Conductivity Caused by Freeze-Thaw: State-of-the-Art, *Hydraulic Conductivity and Waste Containment Transport in Soils, STP 1142*, ASTM, S. Trautwein and D. Daniel, eds., 227-254.

Suter, G. (1993), Compacted Soil Barriers at Abandoned Landfill Sites are Likely to Fail in the Long Term. *Journal of Environmental Quality*, 22 (2), 217-226.

UMTRCA (2013), Uranium Mill Tailings Radiation Control Act Sites. Office of Legacy Management, US Department of Energy, Washington, DC.

Waugh, W., Benson, C., and Albright, W. (2015), Evaluation of Soil Manipulation Methods to Transform Engineered Earthen Covers for Long-Term Waste Containment" *J. Environmental Quality*, doi:10.2134/jeq2015.01.0001.

Yanful E. (1993) Oxygen Diffusion Through Soil Covers on Sulphidic Mine Tailings. *Journal of Geotechnical Engineering*. 119, 1207-1228.

Tables

Table 2.1 Atteberg limits for clays used in this study.

	Liquid Limit	Plastic Limit	Plastic Index
Denver	49	23	26
KF2	41	15	26
New Orleans	29	13	16
Atlanta	50	36	14
Lodgement	18	7	11
Phoenix	27	18	9

Table 2.2 Compaction data used with standard proctor for compacting clay specimens.

	w_{opt}	γ_{dmax}
	%	kN/m3
Denver	18	17.6
KF2	17.5	17.5
New Orleans	12	19
Atlanta	15.5	17.4
Lodgement	9	20.6
Phoenix	8.5	20.5

Figures

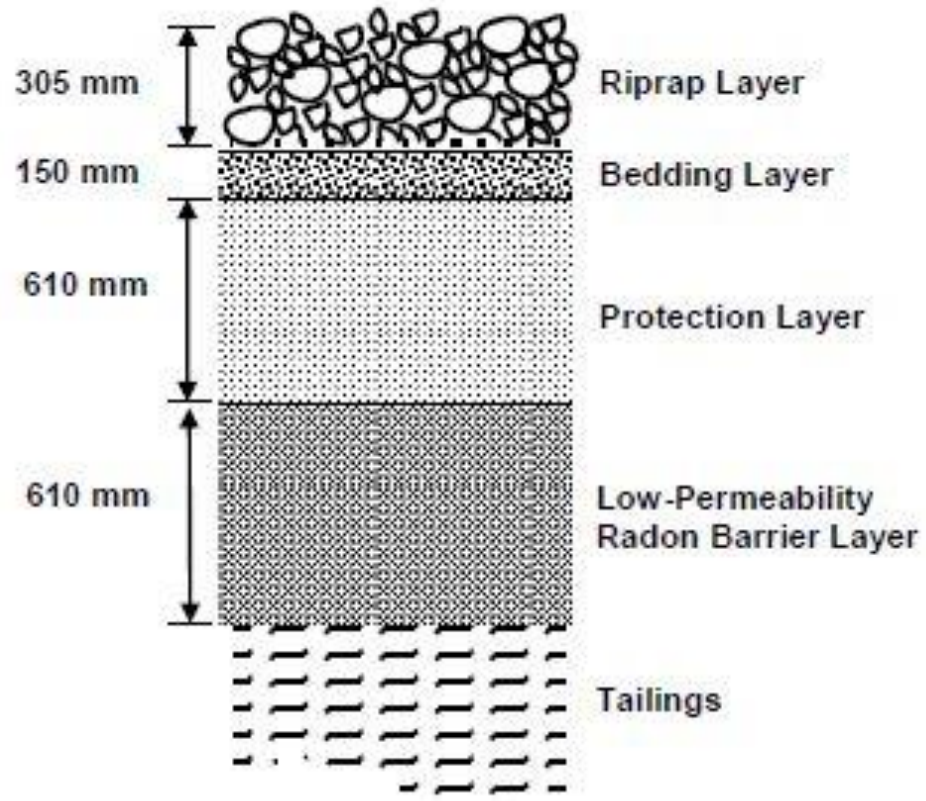

Figure 2.1 General UMTCA design approach for constructing UMTCA disposal cells.

Figure 2.2 Testing apparatus used to provide a solid surface inside the permeamter.

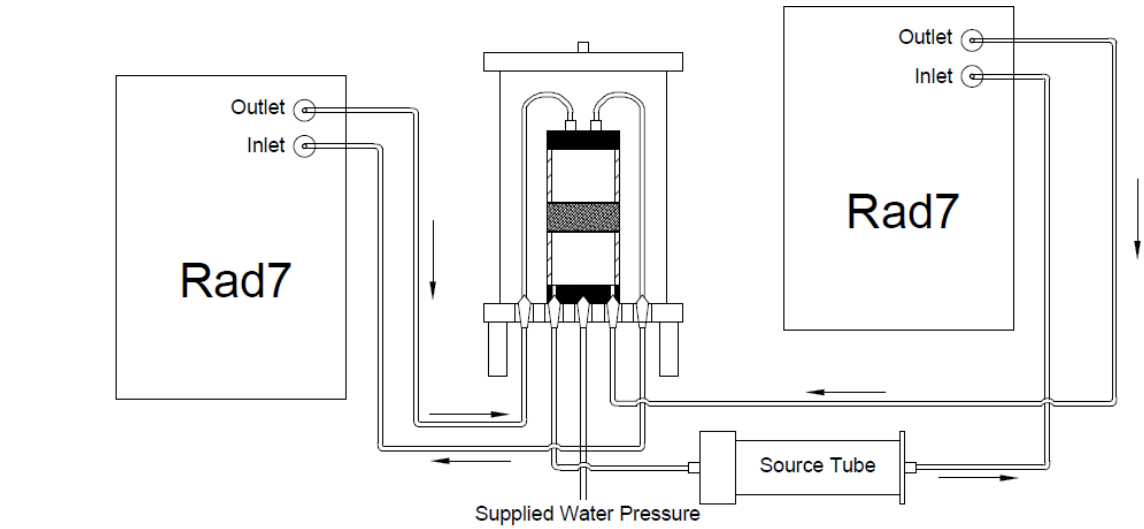

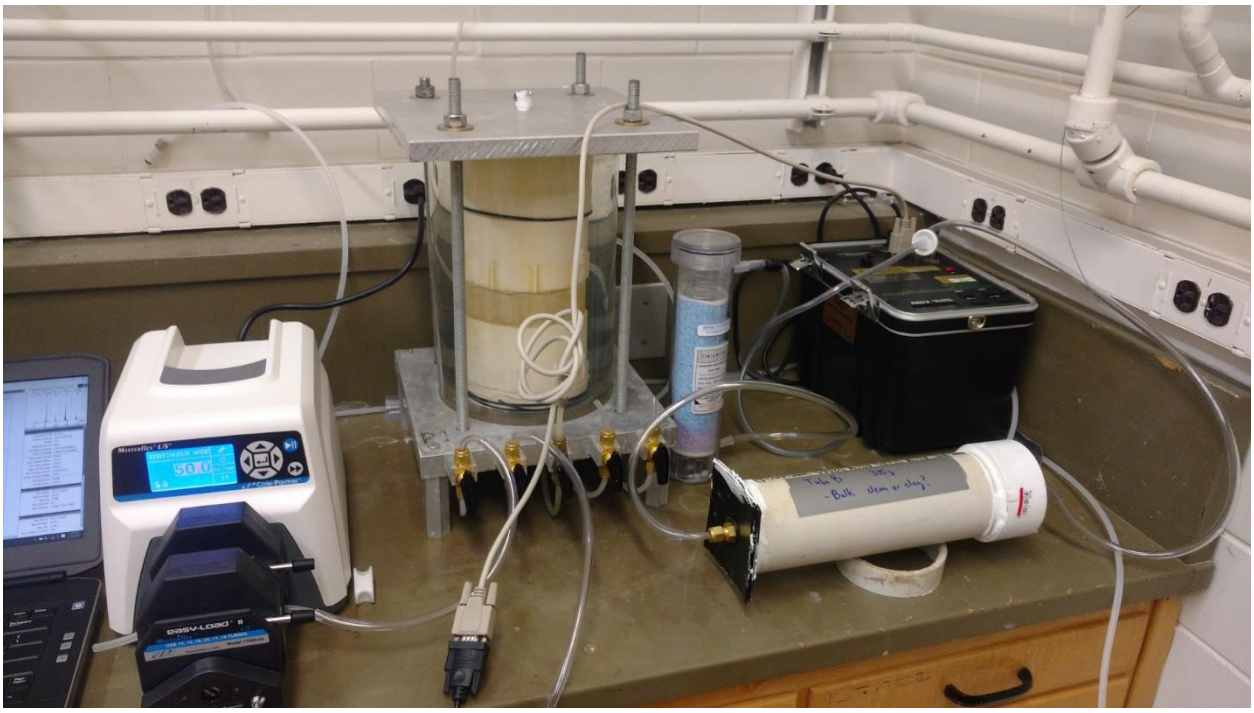

Figure 2.3 Testing schematic (top) of the permeameter adapted to measure D_{Rn}. Air flows from the RAD7 to the corresponding PVC chamber. The right RAD7 samples the source tube that is also exposed to the bottom chamber, creating a constant radon concentration.

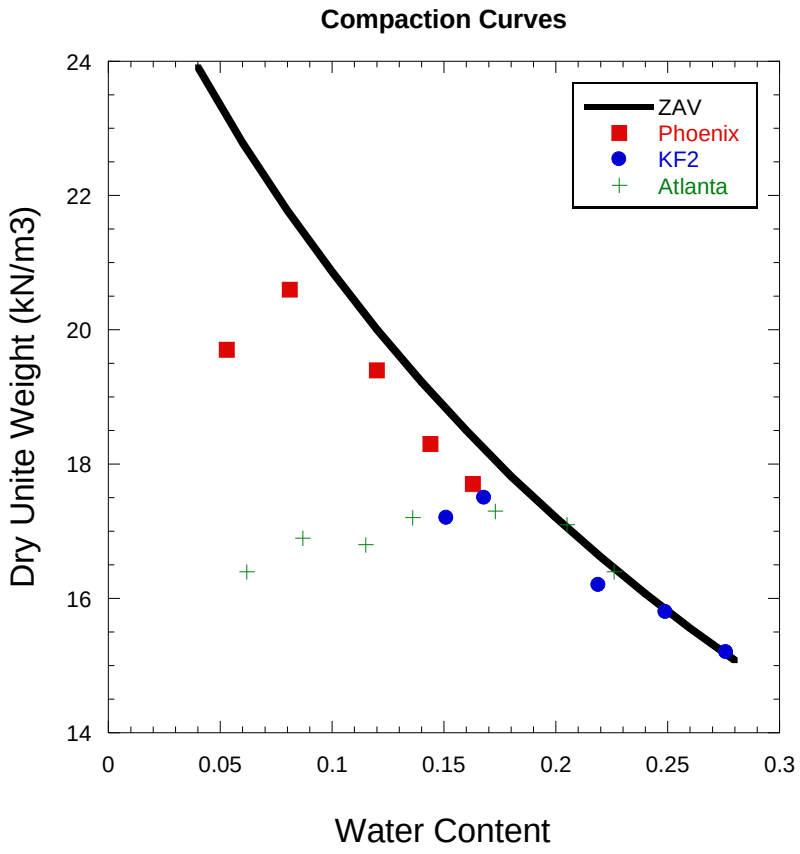

Figure 2.4 Compaction curves for Phoenix, Atlanta, and KF2 clays. The Zero Air Voids curve is the black, solid line. Optimum water content and max dry unit weight was already calculated from previous studies.

Figure 2.5 Three clay samples being prepared to be nearly fully submerged in a desiccator under vacuum to saturate for 24 h.

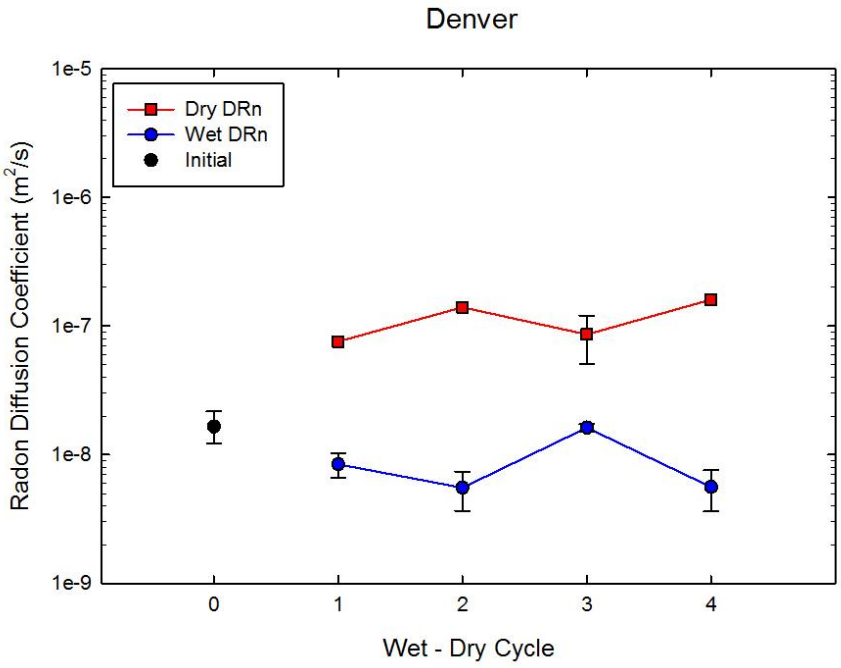

Figure 2.6 Denver effective Radon Diffusion Coefficients.

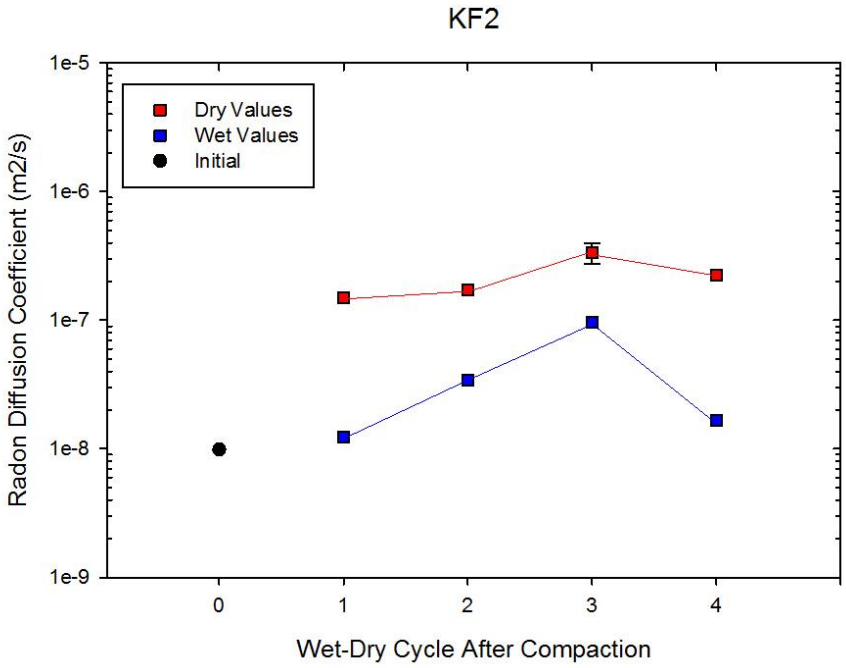

Figure 2.7 KF2 effective Radon Diffusion Coefficients.

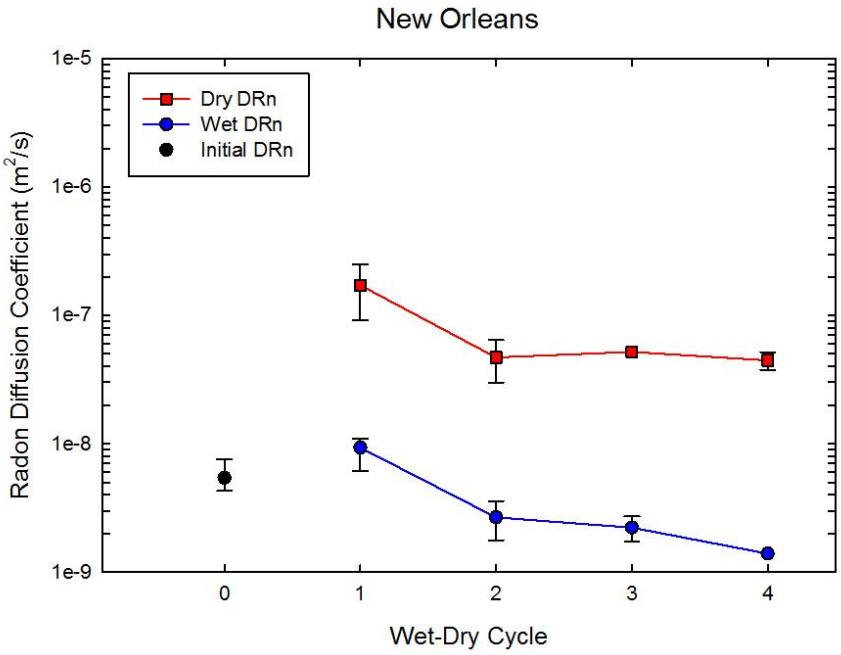

Figure 2.8 New Orleans effective Radon Diffusion Coefficients.

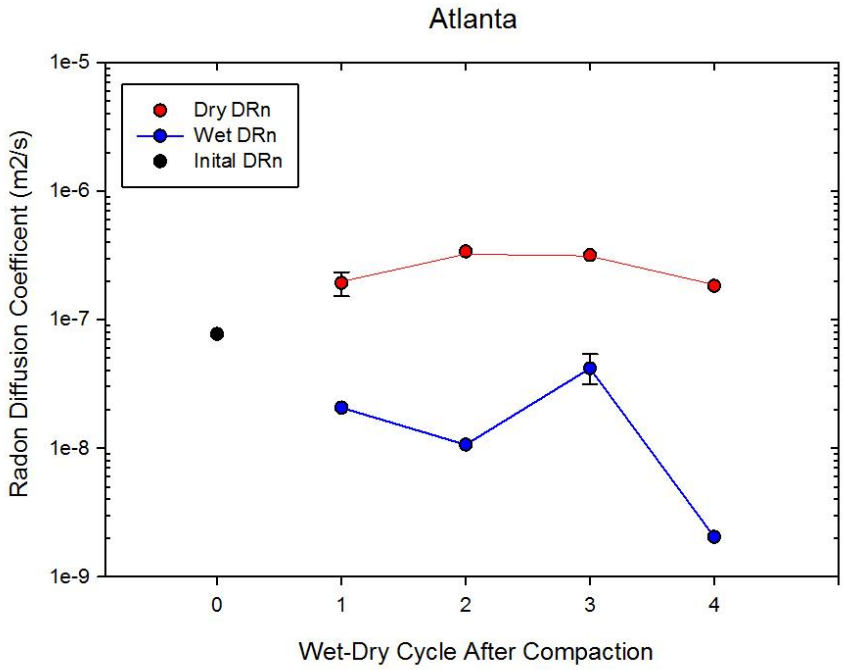

Figure 2.9 Atlanta effective Radon Diffusion Coefficients.

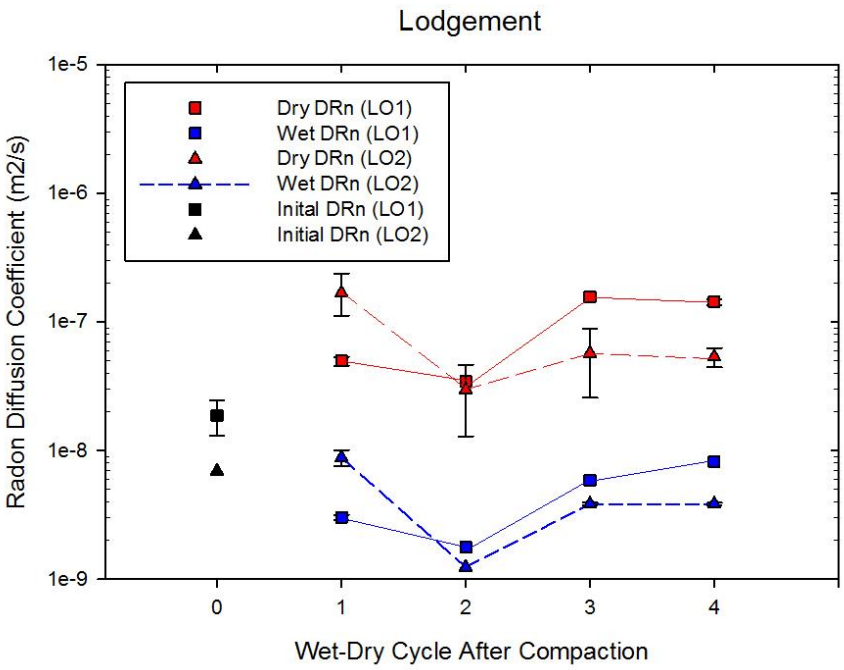

Figure 2.10 Lodgement effective Radon Diffusion Coefficients.

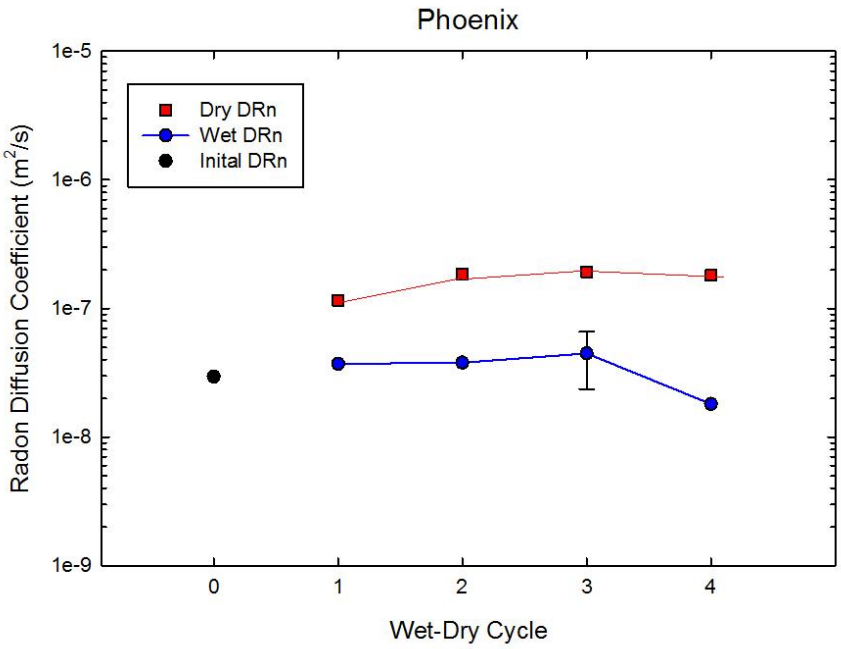

Figure 2.11 Phoenix effective Radon Diffusion Coefficients.

APPENDIX A

2. RADON FLUX MEASUREMENTS AT FALLS CITY, TEXAS

A.1. OBJECTIVE

Measurements taken in this study are part of a larger project scope to compare how compacted clay covers change over long term (>20 years) periods of time driven by environmental factors (e.g. wet-dry cycles, freeze-thaw cycles, bio-intrusion). The Falls City UMTRCA tailings disposal cell in Texas was selected as the first site. Falls City contains higher than average radioactivity and a smaller Radon Barrier (Rn Barrier) thickness compared to other UMTRCA sites. Both traits are desirable for an initial study when the experimental procedure and set up need to be verified.

Different Test Pits were dug in different locations to compare and contrast varying conditions. Flux chambers were installed in each pit so that the Radon flux (Rn flux) emanating through the barrier could be compared. Additionally, activated carbon (AC) canisters were used in tandem with the RAD7 radon monitors to directly relate the two measurement techniques. Lastly, excavation through the Rn barrier was completed to install a flux chamber at top of the tailings. A morphological characterization was also done for each Test Pit but will not be presented here.

A.2. MATERIALS

UMTRCA cover designs typically employ a compacted clay cover about 1 m (3 ft) over the Uranium tailings with a protection layer, typically 0.5 m (1.5 ft), above to limit environmental exposure of wet-dry cycles and root penetration. The Falls City cell closely matches this design. Figure A.1 shows the design thicknesses for each layer at three different locations across the site.

Test Pit locations were selected to contrast the different designed layer thicknesses, surface conditions, and protective layers which will affect long term changes to the Rn barrier. Test Pits span the three different design thicknesses across the site. The top of the cell is covered with shallow grasses (Figure A.2) and intermittent mesquite brush. Mesquite has a woodier and more widespread root structure that has the potential to reach the Rn barrier (Figure A.3). Mesquite is managed and cut each season but its root structure remains even if the surface structures are removed. The top of the cell has the thickest total cover system (Figure A.1.a). Slopes are covered with large stone (about 20 cm on average) that limit vegetative growth (Figure A.4) near the top, the rock top layer flattens out and transitions into the vegetative top slope for about 10 m (30 ft). The design called for a 1 ft rock layer (Figure A.1.b). However, it was discovered to be thicker, about 2 ft. The side slope contains the thinnest cover system, with a 12 in rock layer, 6 in sandy bedding layer, and a 24 in Rn barrier. In 1996, when the Rn barrier was completed, AC flux measurements were conducted in a 100 ft grid and were also used to pick Test Pit locations, prioritizing areas that had higher Rn flux readings.

The same RAD7 (Durridge Company Inc.) measurement devices were used as continuous radon monitors that were used in Chapter 1. AC canisters were also used to measure radon. They were placed inside flux chambers so that the measured radon and corresponding Rn Flux could be compared directly.

Four different Radon flux chambers were used. Similar to Chapter 1, they were named Large, Medium, Small, and Extra Small with the flux areas, A = 2.32 m^2, 0.590 m^2, 0.071 m^2, and 0.018 m^2 respectively (identical to Chapter 1).

A.3. PROCEDURE AND METHODOLOGY

A walkthrough of the Falls City UMTRCA disposal cell was first done to identify where the Test Pits would be located. Post construction AC measurements within the completion report submitted

in 1996 were also used to identify important conditions. Figure A.5 identifies the approximate locations of each Test Pit that was excavated. The Rn flux across the whole site ranged from 0.1 pCi/m^2-s to 4.4 pCi/m^2-s, though the average 0.51 pCi/m^2-s. Table A.1 provides summarized rational for each Test Pit location. Test Pits 1 and 2, 3 and 4, and 5 and 6 where located close, < 8 m, to each other to try and match the same underlying tailings concentration so that the other selected conditions could be compared directly (e.g. presence of woodier vegetation or shallow grass).

Once the Test Pit location was selected, an excavator was used to remove the top soil and protective layer above the Rn Barrier. In most cases, excavation stopped based on a measured depth rather than visual cues because material differences between the protective layer and Rn barrier were extremely difficult to delineate. The surface was then smoothened and flattened as much as possible for installation of the flux chambers.

Four different flux chambers were used, large, medium, small and extra small. All four chambers were sealed with moistened bentonite slurry to prevent Radon leakage under the flux chamber edge. Once sealed, all four chamber sizes were installed with a RAD7 unit to begin measuring the buildup of Radon. Each large and small chamber were given an AC canister to passively adsorb Radon during the time of the measurement. Figure A.6 displays the general set up for each Test Pit at the surface of the Rn Barrier. Buildups where ideally started in the morning and stopped the following morning for an approximate 24 h test. However due to time and logistical restrictions, this was not always possible. Rn fluxes can be calculated with less data points, but the more data, the more reliable and easier the calculation. In some instances, the first test failed either due to RAD7 error or an ineffective seal. When possible the chamber was purged, the seal fixed, and measured again for Rn buildup. These tests were only about five hours in length due to logistical constraints. The methodology and approach to calculating Rn flux from the two measurement techniques was identical to Chapter 1. Several thin wall sampling tubes

were also driven into the Rn barrier. These tubes would later be used to profile water content into the Rn barrier.

Next, a hole was dug through the Rn Barrier big enough for the small flux chamber to be sealed directly on top of the tailings. An AC canister and RAD7 were installed and allowed to build up Radon inside the chamber. Likewise, tests were run for 24 h. But due to logistical and timing constraints tests where occasionally shortened.

Other supplementary tests were also being done in tandem with these Rn flux measurements. Morphological observations in the pedogenisis of the clay cover were conducted by other researchers to further quantify how different Rn Barrier thicknesses or vegetation affect long term soil structure changes in UMTRCA compacted clay covers.

A.4. RESULTS

A.4.1. RAD7 Buildup Curves

In total, six Test Pits with four different sized flux chambers were excavated to compare several different variables that could affect changes in soil structure in the clay cover. Figures A.7 – A.12 contain the buildup curves for each Test Pit (1 to 6 respectively) for each chamber size. The blue data are each measurement taken at the top of the Rn Barrier and the red data are the small chambers that accumulated Radon directly on top of the tailings.

Testing length was designed to be about 24 h. But depending on when the Test Pit was opened during the day, the time of the test could be shortened. In some cases, poor installation of the bentonite seal prevented Radon from building up (Test Pit 1 – extra small and Test Pit 2 – medium) and logistics prevented a second test from being conducted. In other cases, the test length is limited to about five hours. However, all the buildup curves in Figs. A.7 to A.12 contain sufficient data to calculate a flux with both calculation approaches from the RAD7 data.

All RAD7 tests, including the ones conducted at the bottom of the Rn barrier, are summarized in Table A.2. The table also presents AC canister flux measurements completed immediately after the Rn barrier was constructed in 1996. As expected the flux at the top of the tailings (bottom of the Rn barrier) is significantly higher. The flux measurements conducted at the top of the Rn barrier are plotted in Figure A.13.

Because there is no other Rn buildup curve data sets like this on UMTRCA sites, assessing the RAD7 data quality can be challenging. Test Pits 1 to 4 all contain flux measurements higher than any AC tests conducted in 1996. This should not be too alarming as the Rn barrier would have been compacted to optimal water content and have been quite wet, perhaps the wettest it has ever been. Also at that point too, zero structural change had taken place due to wet-dry cycling. Both of the Test Pit 5 and 6 contain significantly lower Rn fluxes but are on the same scale as the 1996 measurements. Not surprisingly, the water content is much higher for these two Test Pit (discussed later). Water content or saturation is a critical component in determining Rn flux and it should be no surprise that the Test Pit with the higher water content contain lower Rn fluxes. The presented Rn fluxes are one data point in time making it difficult to compare directly to the 1996 measurements.

Additionally, an effect of scale due to soil structure is difficult to parse out with this data set alone. However, each flux test has been normalized to account for the large differences in magnitude for all the measured fluxes. All tests run in each tests pit were averaged. The ratio of each Rn flux to its corresponding Test Pit average is plotted in Figure A.14. The one data point that falls outside of the dashed lines was a medium chamber test that produced a noticeably significant low flux. It is presumed that this test was not sealed adequately and that the calculated flux is not representative of the actual flux present at that time. When testing was going on, it was documented and observed that the medium chamber wall was less rigid than the other chambers.

This same issue led to a failed medium chamber test in Test Pit 2 and it is not unreasonable to suspect that a similar issue occurred with this medium chamber in Test Pit 4.

The standard deviation of data can also be compared directly with the normalization of concrete tests run in the laboratory in Figure A.14. Concrete tests have been normalized to the average flux of the concrete slab. As expected, the field measurements have quite a bit more spread and variability than the much more homogenous and isolated concrete slab. After normalization, the concrete slab had population standard deviations of 0.37, 0.20, 0.14, and 0.09 for the extra small, small, medium, and large chambers respectively. The field Rn flux chambers are 0.95, 0.35, 0.52, and 0.42. Both sets of data show downward trends in standard deviation while, as expected, the field measurements are larger due to the significantly more heterogeneous composition of the compacted clay layer.

A.4.2. Activated Carbon Canister Measurements

AC canisters were run in tandem with RAD7 buildup curves, but not all buildup curves were reliable enough to compare to AC directly. In several instances, the Rn concentration built up normally but then dropped suddenly, only to rise back up again. It is expected that nightly storm fronts supplied pressure changes affected the transport of Rn from the tailings into the flux chamber. It would be inappropriate to attempt to directly compare the end RAD7 data to the AC canister concentration. Similarly, second tests were run inside flux chambers due to RAD7 errors or poor bentonite seals that leaked too much radon. Rn fluxes where still calculated from the RAD7 because the whole curve is not needed; only the initial points in the buildup curve. But for AC methods, they cannot be used with any degree of confidence.

The six successful tests are summarized in Table A.3. The AC to RAD7 Rn Concentration ratio ranged from 0.49 to 0.69 with an average of 0.60. This range and average agrees well with

laboratory measurements discussed in Chapter 1. Even in the field measurements, there appears to be a systematic biasing where AC canisters consistently measure less radon then the RAD7.

Figure A.15 presents the AC and RAD7 buildup data for three of the discussed tests. The blue data - RAD7 build up show a decrease in concentration near the end of the test. This was due to a low battery in the RAD7 unit and the max value of Rn concentration was presumed to be the actual concentration inside the flux chamber. The results agree well with the similar laboratory tests.

Upon review of the data, it is clear that the AC data, as analyzed by RTCA and as presented here, should not be used to determine Rn flux. To determine Rn flux with one data point at the end of an exposure period, it must be assumed that the buildup curve is linear. This slope can then be used identically to the M_e approach in calculating a flux with RAD7 data. In practicality, Eq. 7 from Chapter 1 achieves the same thing and is used to convert the AC data into flux data.

Figure A.16 show the initial slope for the RAD7 data and the assumed linear buildup measured with AC. For Test Pit 6, the large chamber, the slopes are 398.2 and 171.6 Bq/m^3-h. Those values correspond to 0.59 and 0.195 pCi/m^2-s respectively. The other six successful Rn flux comparisons are summarized in Table A.3. At best, the AC to RAD7 Rn flux ratio is 0.38, a significant difference in observed flux. As could be expected, the two large chamber tests performed better (0.24 and 0.38) than the small chambers with an average ratio of 0.07, nearly a full magnitude of difference. Large chambers take longer to be affected by back diffusion and maintain the linear regime longer than small chambers. AC canisters have severe limitations in the lab analysis and procedure used here but because the Rn concentration is systematic, corrections can be used to provide more accurate data measurements.

A.4.3. Water Content Profile

Two to three Shelby tubes where driven into the top of the Rn barrier to collect water content data. Clay pucks, about 30 mm were extruded and assessed for gravimetric water content according to ASTM D2216 – 10. All six profiles are summarized in Figure A.17. Paired Test Pits are similar shades of color and generally agree well with each other. The high degree of scatter in TP 1A, 2A, and 4A is expected to be due to pre-existing clay structure from the burrow source for the Rn Barrier.

It was observed that much of the original clay structure in the borrow source was still intact. Clumps (as big as 50 mm in diameter) could easily be identified within the Rn barrier. When the barrier was constructed, this burrow material was not kneaded enough and is has distinct material properties compared to the rest of the barrier, water content being one of them. Additionally, this orginal structure was much higher strength and made it difficult to impossible to maintain clean cuts of clay pucks when extruding the Shelby tubes. As a result, it was difficult to get accurate bulk unit weight data.

Finally, some roots were observed in two of the Shelby tubes sampled through the Rn barrier. Small roots (about 1 mm in thickness) were observed in the first 30 mm of tube TP1A (Figure A.18). They were also found throughout the whole profile of TP3A. TP3A also had a few large roots (5 mm in thickness) found 150 mm deep into the tube (Figure A.19). Perhaps because clear evidence of roots, the slight increase in average Rn flux from Test Pit 1 to Test Pit 2 and much large increase in Rn flux from Test Pit 3 and Test Pit 4 can be attributed to this bio intrusion.

A.5. CONCLUSIONS

Field measurements were conducted to evaluate Rn flux under several different conditions the Rn barrier is exposed to. Four different chamber sizes where used to compare scale effects and determine best variability in collected data. AC canisters were used in tandem with several RAD7 measurements to compare the two measurement techniques. Based on the collected data, several conclusions can be made.

The RAD7 experimental set up can be used to effectively and reliably to measure Rn flux. This approach provides a continuous buildup in concentration that provides more data and a superior window into calculating Rn flux that AC cannot provide. More data is needed to have a higher degree in confidence in the scaling effects observed. But, they follow the same pattern as lab data. With this data set, Test Pit 1 (and to a lesser extent Test Pit 3 and 5) demonstrate that as the chamber size decreases, the Rn equilibrium concentration increases, also congruent with lab data. Additionally, normalizing flux values to the Test Pit average shows that the larger the chamber, the less variability with repeated measurement, also identical to laboratory results. Finally, the presence of woodier, deeper penetrating root systems do slightly affect Rn flux when those roots penetrate the Rn barrier as observed with comparing Test Pits 1 and 2 and Test Pits 3 and 4.

AC used as a measurement technique must be properly calibrated to be used reliably. Clearly, there appears to be a systematic error of AC measuring less radon then RAD7 (the AC to RAD7 Rn concentration ratio averaged 0.60). This is consistent with similar laboratory measurements and possibly stems from a kinetic delay or inappropriate use of correction factors. As radon flushes into the chamber, it takes time before it is properly equilibrated with the AC. From reviewing the AC measurements conducted after the Rn barrier was initially constructed in 1996, it does appear that calibration to a standard was done for their measurements. However, each flux chamber experienced significant back diffusion well after 7 h in ever flux chamber. The

longer the test, the shallower the slope and less accurate it gets from the actual flux that can be reliably calculated from the RAD7 buildup curves. Even if the radon concentration perfectly matches the RAD7 data, the flux will still be inaccurate when compared to the RAD7 data. From this data set, it would be recommended that AC tests should not run past 7 h, though this could be adjusted depending on the chamber size and initial Rn flux.

TABLES

Table A.1 Test Pit conditions selected to be compared. Test Pits 1 and 2, 3 and 4, and 5 and 6 where located spatially very close, > 10 m, so they could be compared directly.

Test Pit	Condition		
	Vegetation	Tailings Concentration	Designed Cover System
1	Mesquite	Higher than site average (1.0-4.0 pCi/m^2-s)	Top of Cell (Figure A.1.a)
2	Shallow Grasses	Higher than site average (1.0-4.0 pCi/m^2-s)	Top of Cell (Figure A.1.a)
3	Mesquite	Site Average (~0.5 pCi/m^2-s)	Top of Cell (Figure A.1.a)
4	Shallow Grasses	Site Average (~0.5 pCi/m^2-s)	Top of Cell (Figure A.1.a)
5	None: Rip Rap	Higher than site average (1.0-4.0 pCi/m^2-s)	Top of Slope (Figure A.1.b.)
6	None: Rip Rap	Higher than site average (1.0-4.0 pCi/m^2-s)	Side Slope (Figure A.1.c.)

Table A.2 Summary of all Radon Flux Measurements taken at Falls City.

Test Pit	Chamber Size	Radon Flux [pCi/m2-s]		
		"As Built"	2016	Tailings 2016
1	Large	3.00	4.11	52.11
	Medium		10.06	
	Small		14.49	
	Extra Small		DNW	
2	Large	3.00	7.57	55.62
	Medium		DNW	
	Small		8.74	
	Extra Small		4.56	
3	Large	0.30 - 0.90	9.03	139.22
	Medium		24.01	
	Small		11.96	
	Extra Small		24.74	
4	Large	0.30 - 0.90	1.08	7.14-41.52*
	Medium		0.38	
	Small		4.19	
	Extra Small		7.29	
5	Large	1.00 - 4.00	0.14	DNW
	Medium		0.20	
	Small		0.24	
	Extra Small		1.23	
6	Large	1.00 - 4.00	0.52	1148.07
	Medium		0.53	
	Small		0.35	
	Extra Small		0.06	

DNW = Did not work. The bentonite seal for two tests did not properly contain Radon and therefore no build up was measured.

*The poor quality of data limited accuracy in calculating a Radon Flux and an upper and lower range of Radon fluxes are presented.

Table A.3 Summary of reliable AC-RAD7 direct comparison measurements.

Test Pit	Chamber	AC Concentration		RAD7 VALUE	Ratio AC/RAD7 Rn Concentration	Ratio AC/RAD7 Rn Flux
		[pCi/L]	[Bq/m3]	[Bq/m3]		
1	Large	418.8	15497	27000	0.57	0.24
1 - Bottom	Small	966.2	35750	73400	0.49	0.14
2	Small	195.1	7220	10400	0.69	0.06
4 - Bottom	Small	195.4	7228	11800	0.61	0.02
6	Large	76.5	2831	4480	0.63	0.28
6 - Bottom	Small	31097.1	1150594	1930000	0.60	0.05

FIGURES

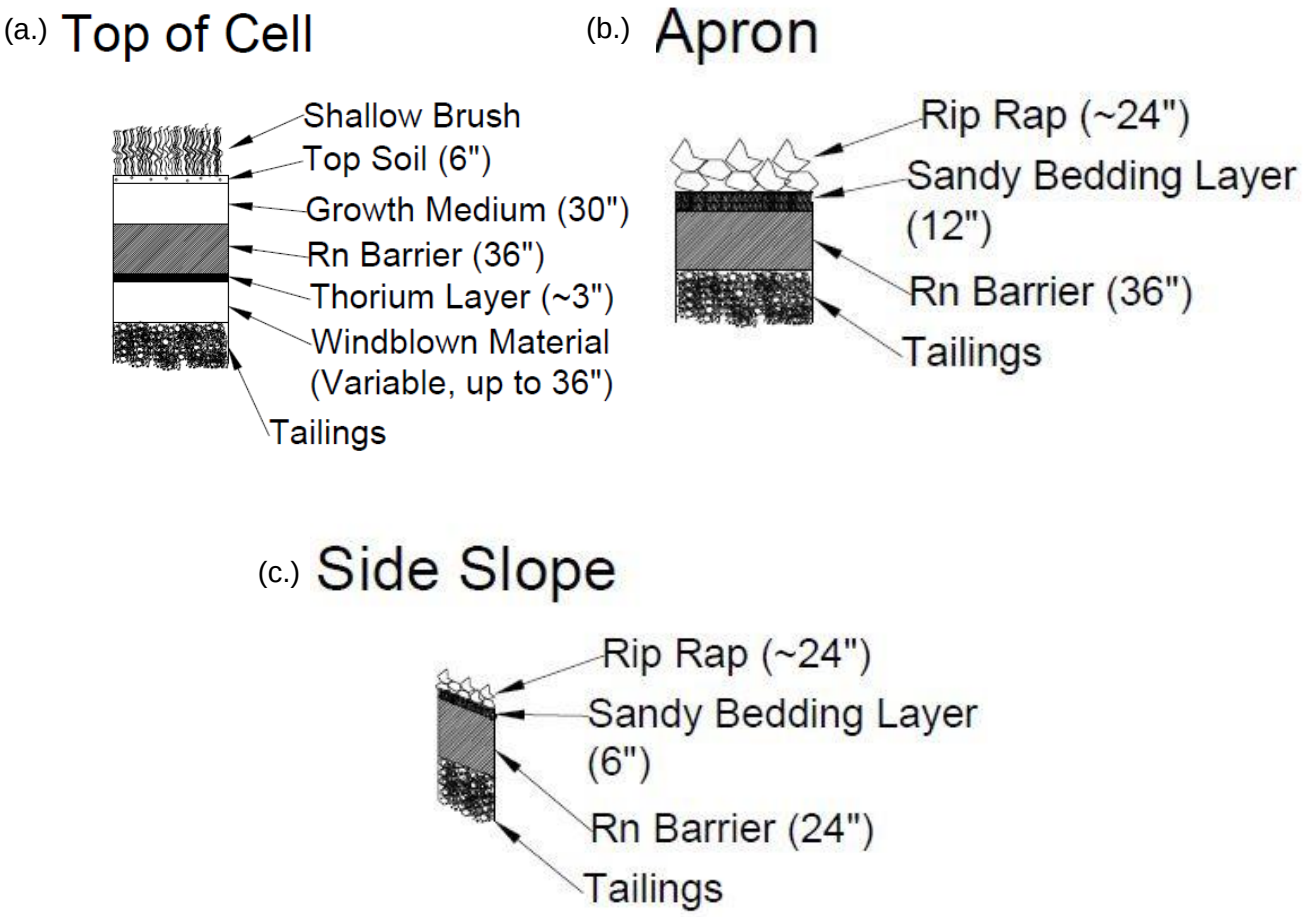

Figure A.1 Design Cross Section for the Falls City, TX UMTRCA cover system: (a.) top of cell, (b.) slope apron, and (c.) side slope.

Figure A.2 Shallow grasses that cover the Falls City disposal cell. The right part of the picture shows mowed grass.

Figure A.3 Woodier vegetation at the surface (mesquite brush) can be seen in clusters.

Figure A.4 The top figure shows the transition from the vegetative cell cover to the rock apron. The bottom image looks up the rock armored slope.

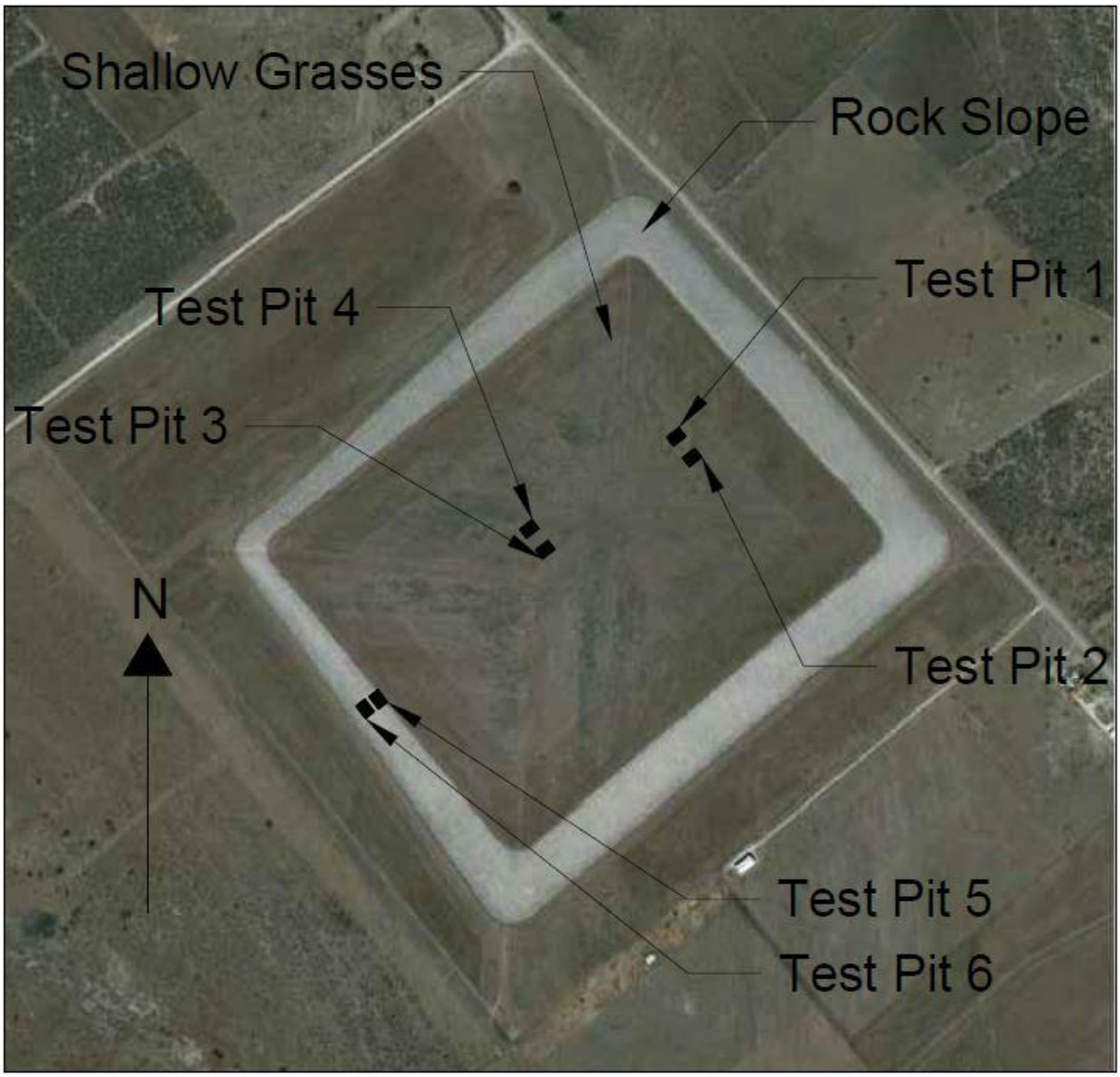

Figure A.5 Aerial view of the Falls City UMTRCA cell with each approximate Test Pit location identified.

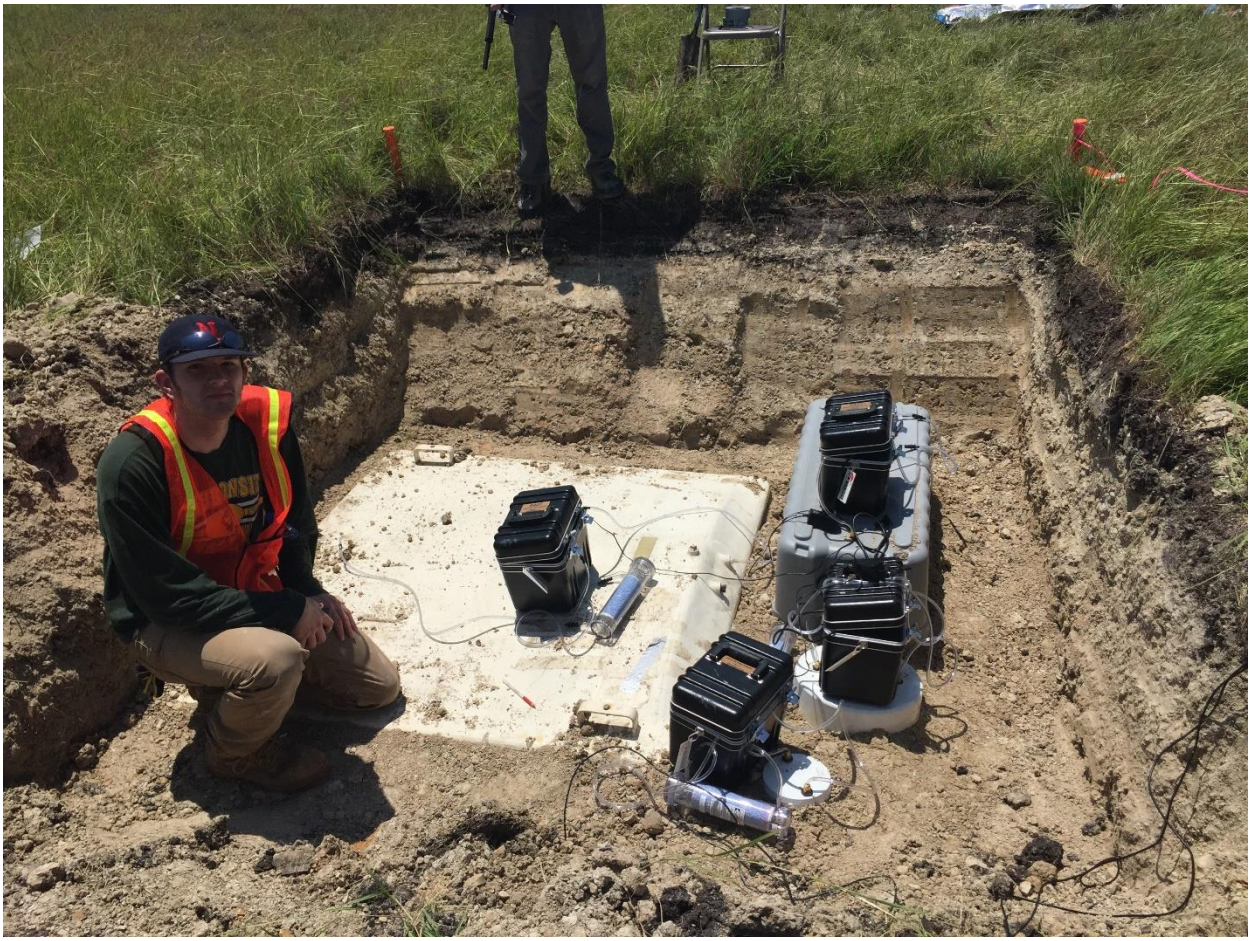

Figure A.6 General layout of each Test Pit with the large, medium, small, and extra small chambers measured Rn build up curves at the top of the Rn Barrier.

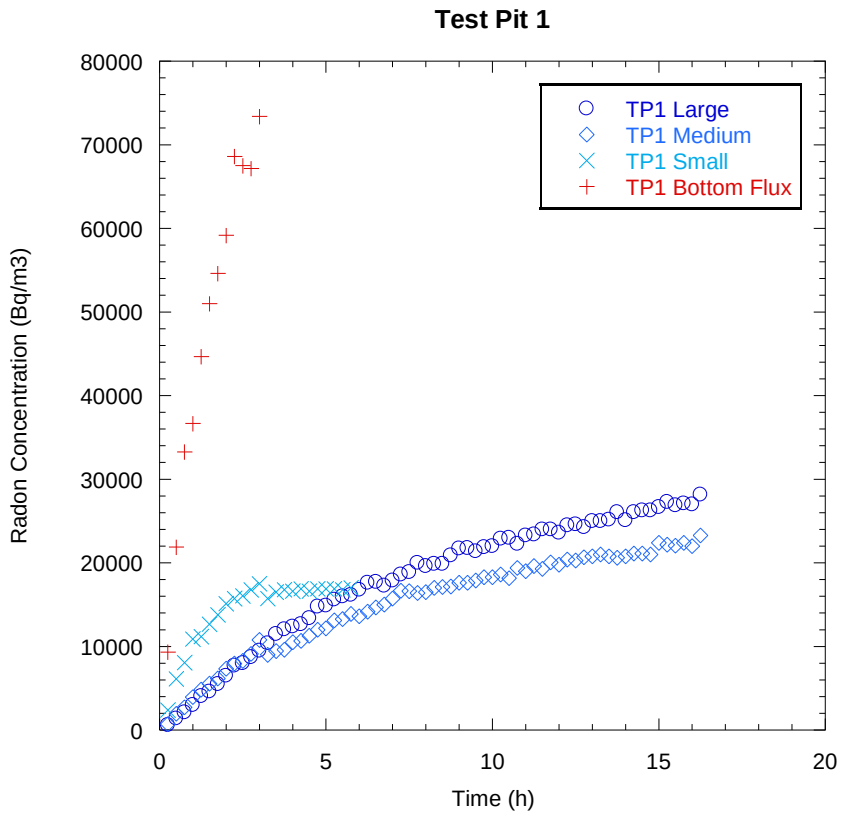

Figure A.7 Radon build up curves measured in Test Pit 1 are plotted together.

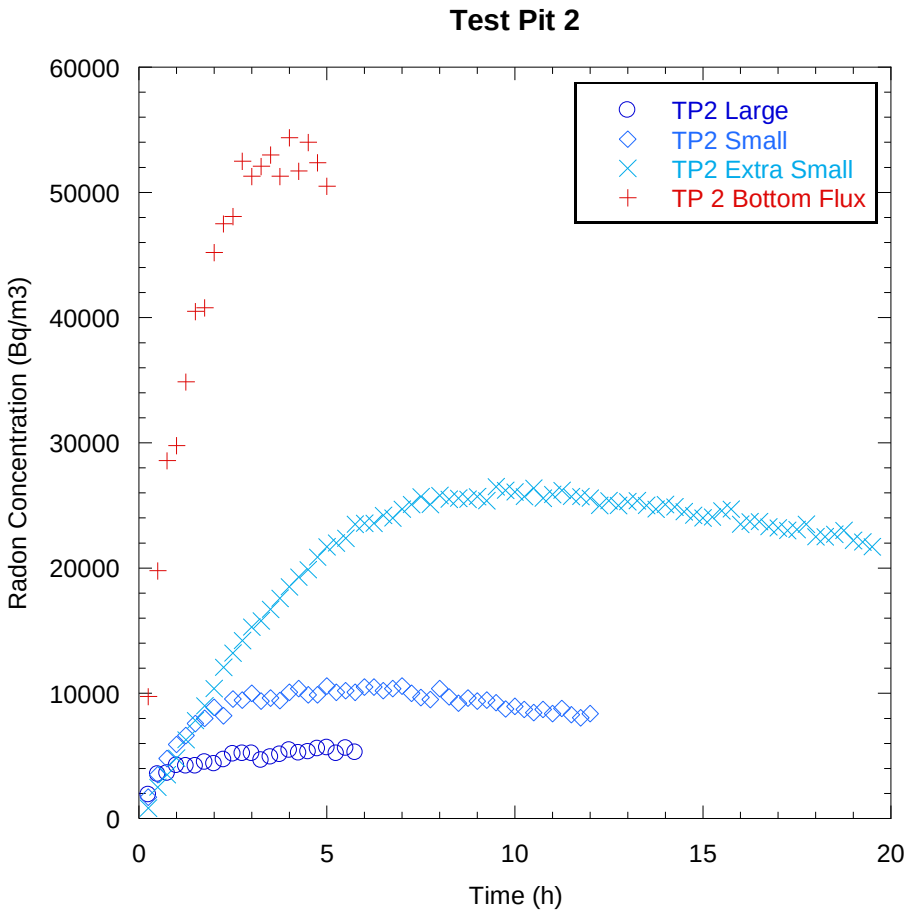

Figure A.8 Radon build up curves measured in Test Pit 2 are plotted together.

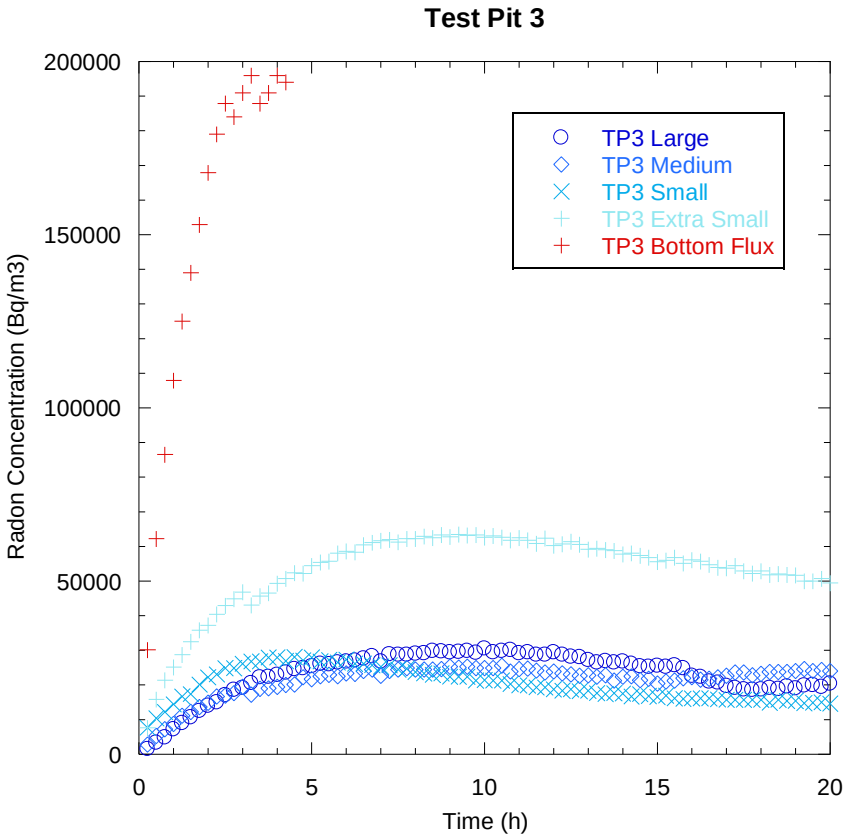

Figure A.0.2

Figure A.9 Radon build up curves measured in Test Pit 3 are plotted together.

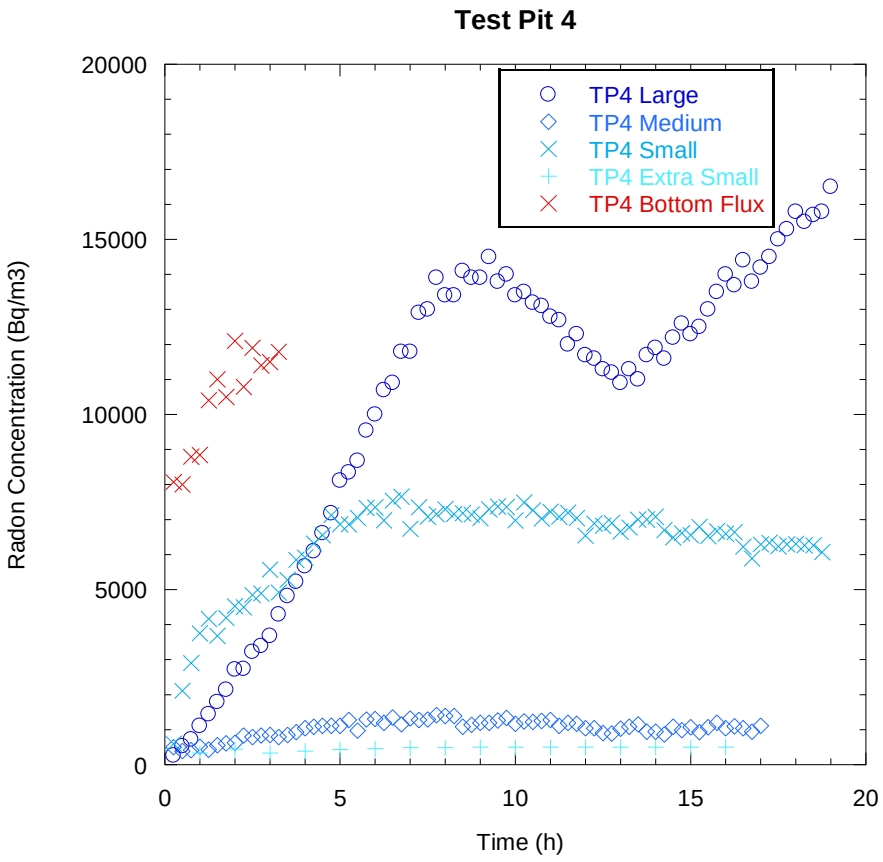

Figure A.0.3

Figure A.10 Radon build up curves measured in Tit Pit 4 are plotted together. The abnormal rise and fall of the large chamber buildup curve is expected to be due to a large drop in ambient air pressure from a storm front that moved in after installation.

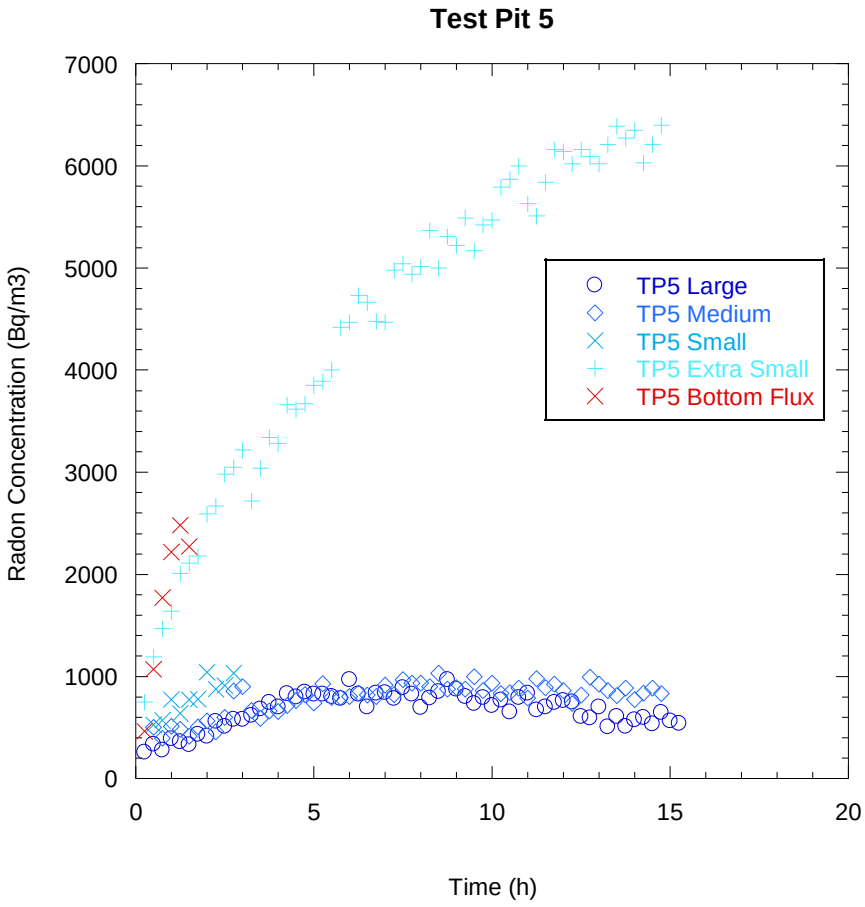

Figure A.11 Radon build up curves measured in Test Pit 5 are plotted together.

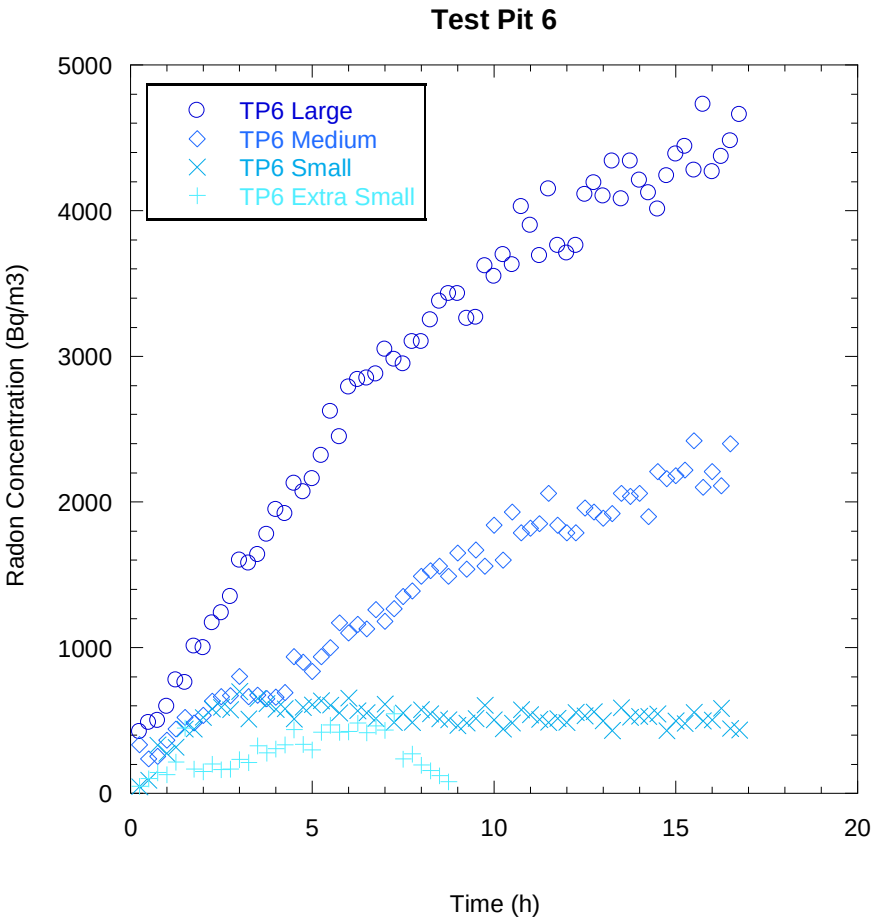

Figure A.12 Radon build up curves measured in Test Pit 6 are plotted together.

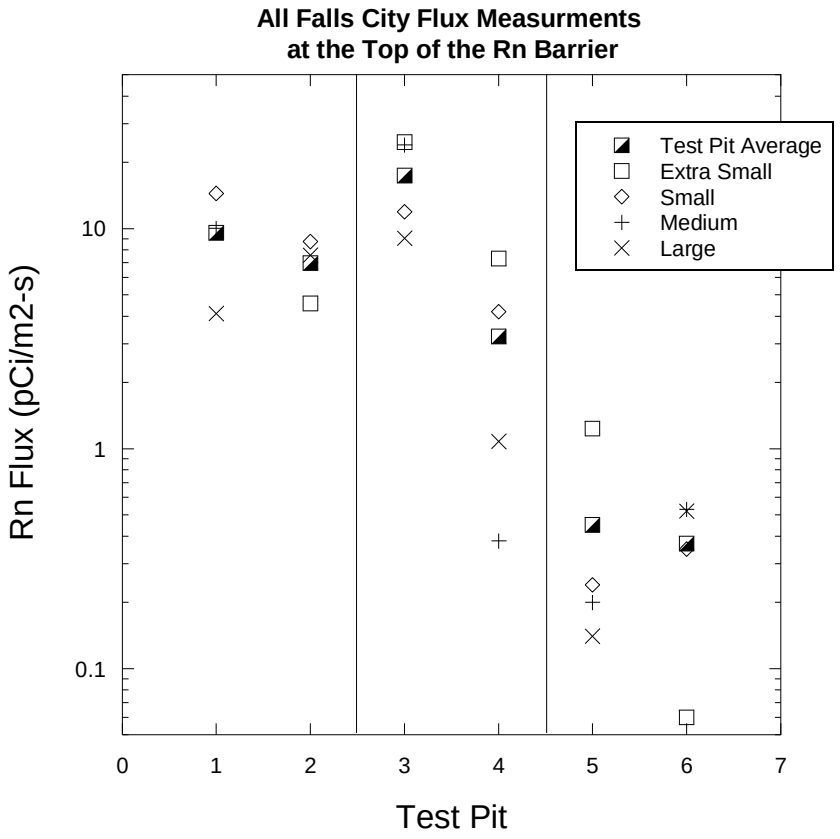

A.13 All Rn flux measurements taken at Falls City from April 25th to 29th.

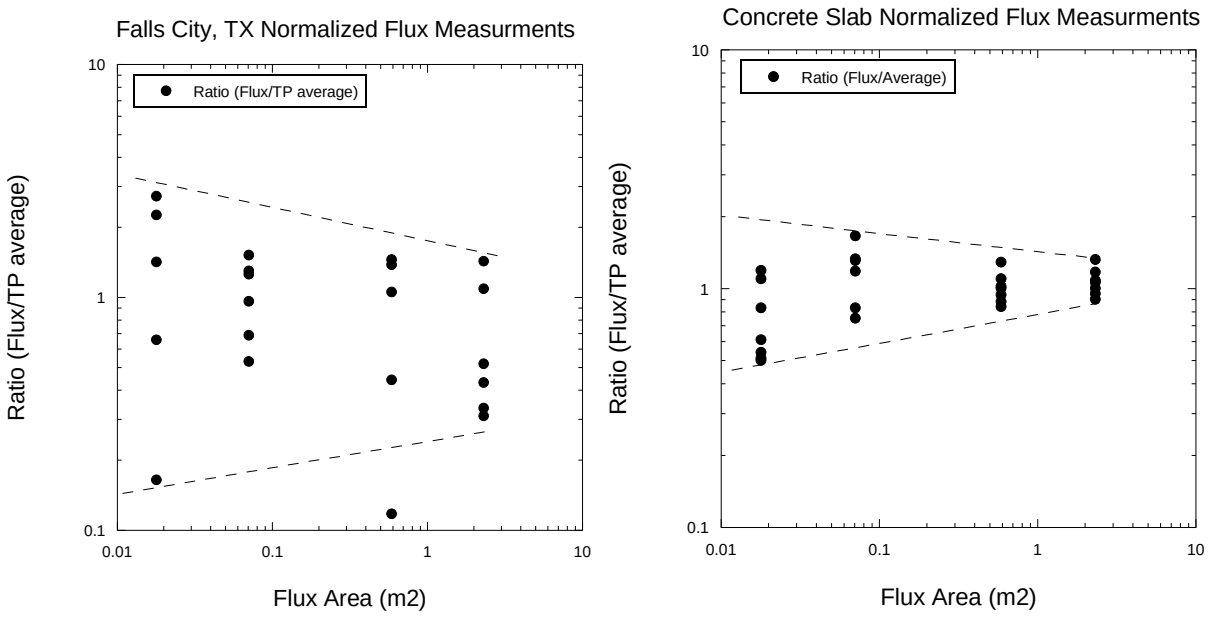

Figure A.14 (Left) From the Falls City field data, each flux value has been normalized by averaging the 4 flux measurements in each Test Pit. Each flux was then rationed by its Test Pit average. (Right) The laboratory flux ratios to the average over all flux measurements from Chapter 1.

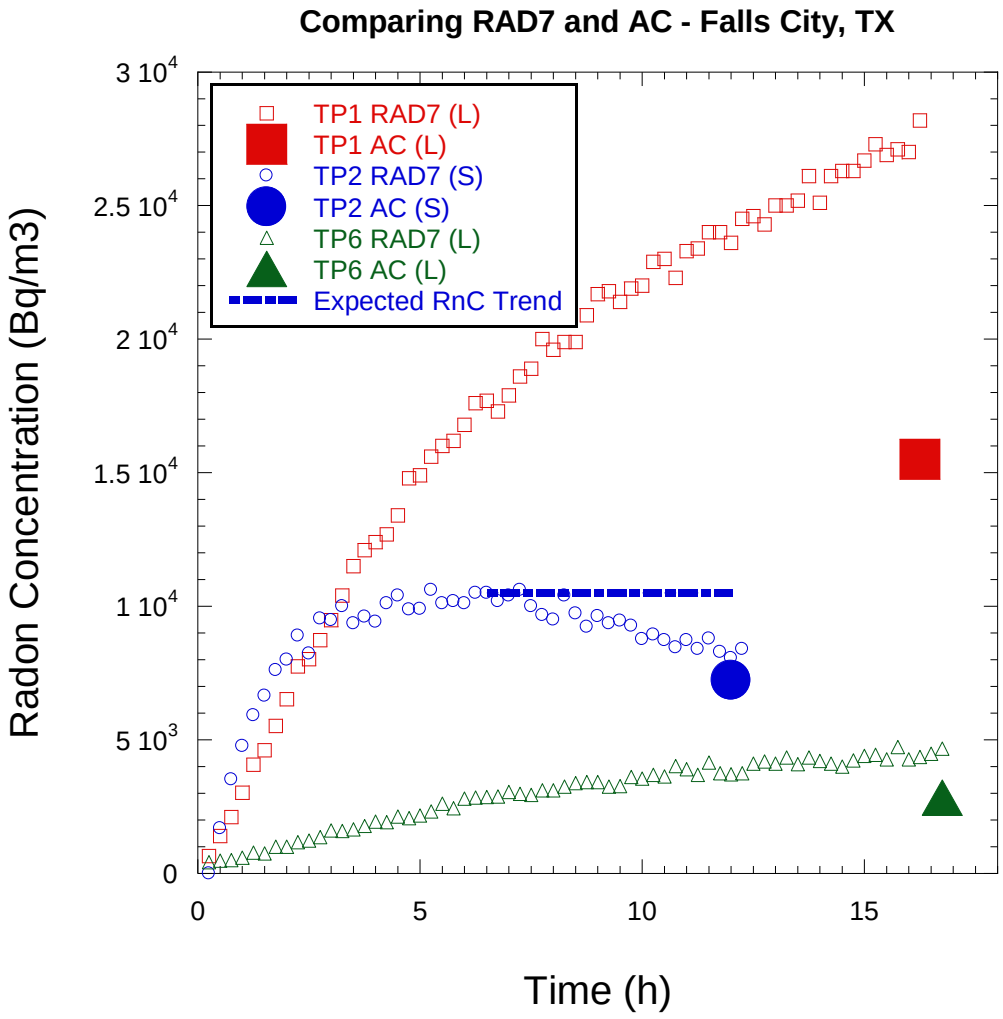

Figure A.15 Three Rad7 (small open data points) and AC (single large filled data point) flux test data.

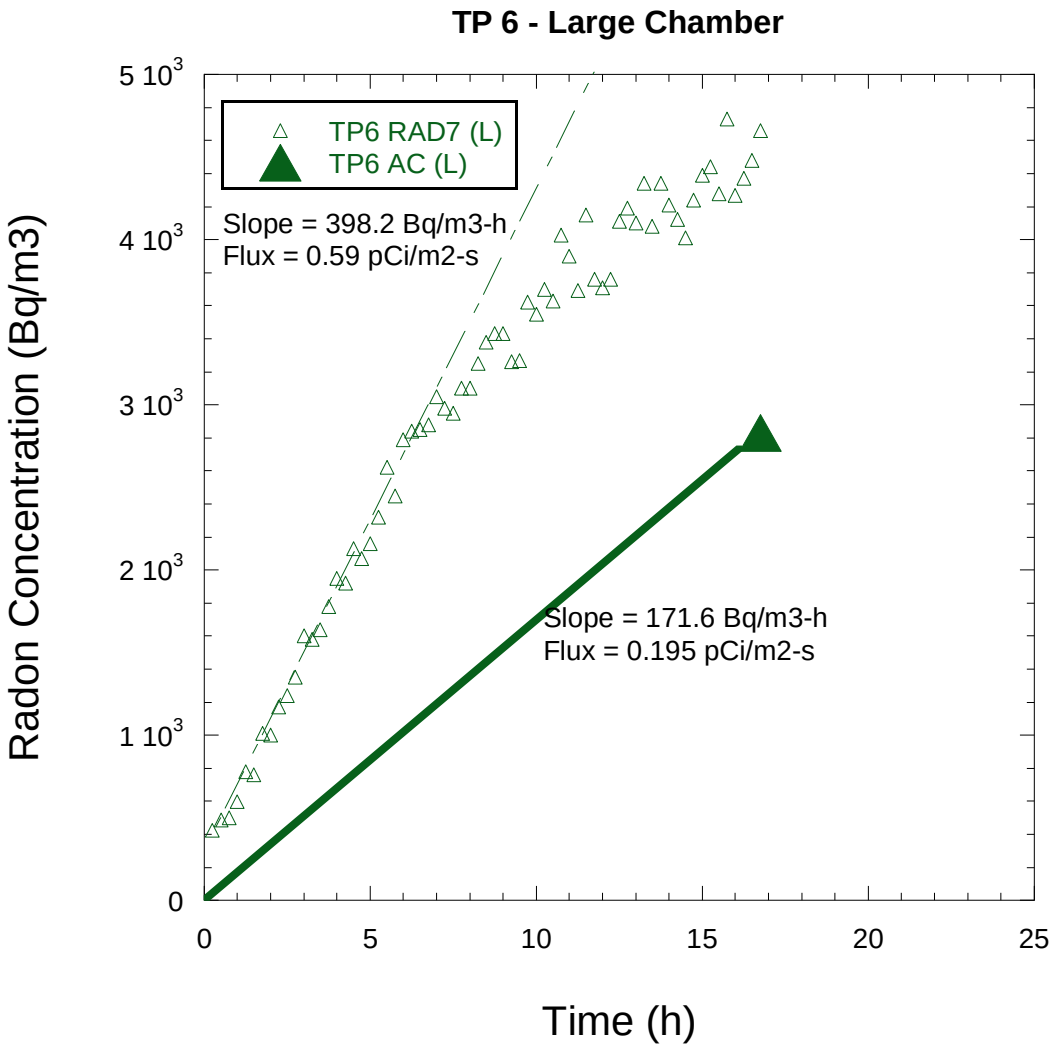

Figure A.16 Comparing the slopes and flux calculation for AC and RAD7 data for the large chamber in Test Pit 6.

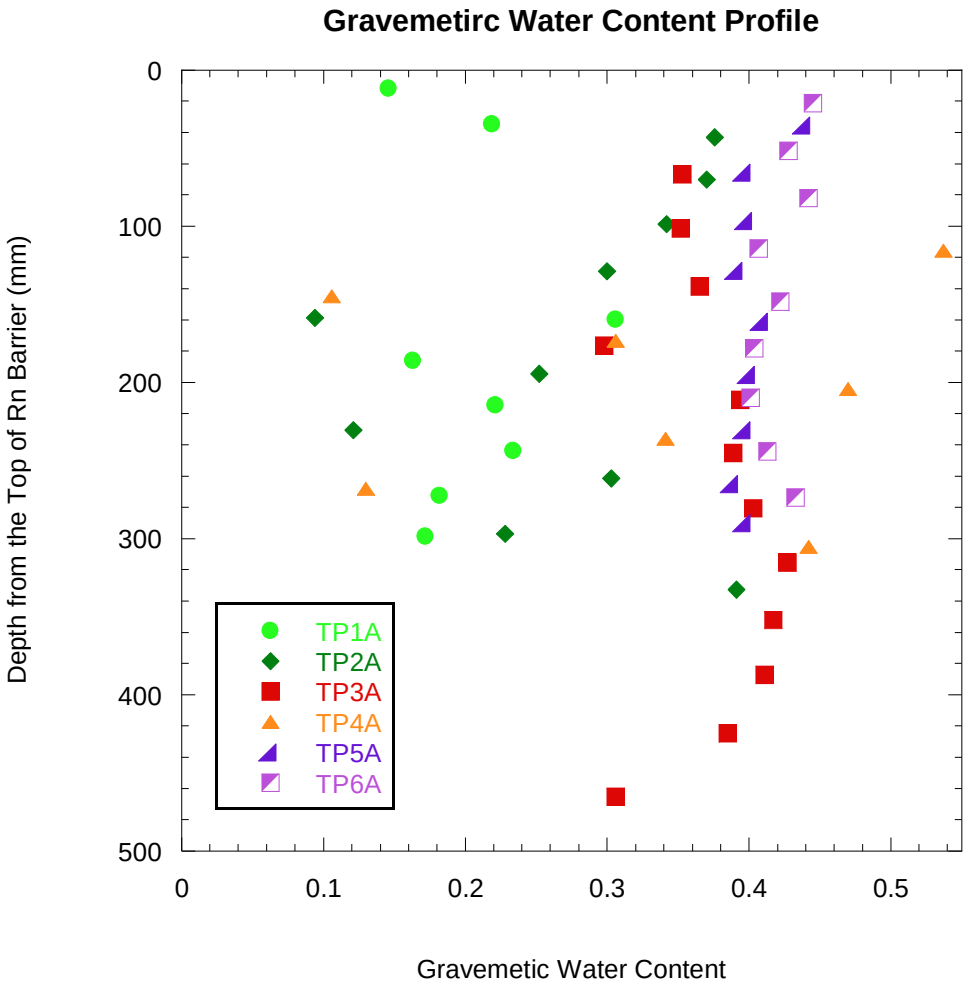

Figure A.17 Water content profiles derived from ASTM D2216 -10 and Shelby tube sampling from the top of the Rn barrier.

Figure A.18 Smaller roots, only 1 mm in thickness observed in the top of TP1A tube and throughout TP3A tube.

Figure A.19 Larger mesquite brush roots found in TP3A tube found 150 mm deep into the Rn barrier. Roots are about 5 mm in thickness.